Polystyrene Upcycling into Fungal Natural Products and a Biocontrol Agent

Chris Rabot,[†#] Yuhao Chen,[‡§#] Shu-Yi Lin,[†] Ben Miller,[†‡] Yi-Ming Chiang,[†] C. Elizabeth Oakley,[‖] Berl R. Oakley,[‖] Clay C. C. Wang,[†‡§*] & Travis J. Williams[‡§*]

[†]Department of Pharmacology & Pharmaceutical Sciences, University of Southern California, 1985 Zonal Ave, Los Angeles, CA 90089.

[‡]Donald P. and Katherine B. Loker Hydrocarbon Institute and Department of Chemistry; 837 Bloom Walk, University of Southern California, Los Angeles, CA 90089.

[§]Wrigley Institute for Environmental Studies, 3454 Trousdale Parkway, Los Angeles, CA 90089.

[‖]Department of Molecular Biosciences, University of Kansas, 1200 Sunnyside Avenue, Lawrence, KS 66045.

[#]These authors contributed equally to this work.

*Corresponding authors. Emails: clayw@usc.edu, travisw@usc.edu

KEYWORDS plastic upcycling, polystyrene, catalysis, synthetic biology, biosynthesis, genetic engineering

ABSTRACT: Polystyrene (PS) is one of the most used, yet infrequently recycled plastics. Although manufactured on the scale of 300 million tons per year globally, current approaches toward PS degradation are energy- and carbon-inefficient, slow, and/or limited in the value that they reclaim. We recently reported a scalable process to degrade post-consumer polyethylene-containing waste streams into carboxylic diacids. Engineered fungal strains then upgrade these diacids biosynthetically to synthesize pharmacologically active secondary metabolites. Herein, we apply a similar reaction to rapidly convert PS to benzoic acid in high yield. Engineered strains of the filamentous fungus *Aspergillus nidulans* then biosynthetically upgrade PS-derived crude benzoic acid to the structurally diverse secondary metabolites ergothioneine, pleuromutilin, and mutilin. Further, we expand the catalog of plastic-derived products to include spores of the industrially relevant biocontrol agent *Aspergillus flavus* Af36 from crude PS-derived benzoic acid.

INTRODUCTION

Plastic polymers have delivered immeasurable benefits to society. Attributable to their variable densities, plasticities, and other physicochemical properties, they have been extensively applied to virtually every industry today. The profound benefits conferred by plastics necessitate that they will remain an integral part of our economy. It is therefore imperative that we continue to develop an expanding portfolio of diverse and effective methods to maximize the value that we reclaim from them at the end of their first use.

Polystyrene (PS) is one of the most common, but least frequently recycled plastics. Current recycling rates of PS are extremely low; only 0.9% of PS was recycled in 2018 in the United States.[1] PS is manufactured in several forms: about 10% is expanded polystyrene foam (EPS), 50% is pure PS, and the remaining 40% is blended with other plastics to form copolymers.[2] These different forms of PS have widely varied densities, from 0.016 to 1.04 g/cm3,[3] and as a result, they create complications in waste sorting when they are managed in recycling centers. Attributable to its highly stable and hydrophobic chemical structure, natural PS degradation is extremely slow.[4,5]

Taken together, the volume of PS manufacturing, slow environmental degradation rate, and complex recycling challenges lead to its abundance both in landfills and the environment, the latter ultimately arriving in the oceans. In fact, PS occupies approximately one-third of landfills worldwide,[6] and leaked PS waste in the environment[7,8] cause adverse health effects both to humans[9-12] and wildlife.[13-15]

Several groups have recently reported methods to convert PS to fine chemicals, such as graphene[16] and styrene[17]. In the past year, multiple groups have independently reported the conversion of PS to benzoic acid (BA).[18-21] In addition to chemical upcycling approaches, biological solutions to plastic degradation have also been of increasing interest. Several fungal[22,23] and bacterial[24-26] species have been shown to degrade PS or related polymers. Mealworms can also consume PS.[27,28] Two groups have shown that *Pseudomonas putida* can convert styrene to biodegradable polyhydroxyalkanoates (PHAs).[29,30] Recently, one group showed that mixed plastics, including PS, can be oxidatively degraded and upgraded by an engineered strain of *P. putida* to β-ketoadipate or PHAs.[31]

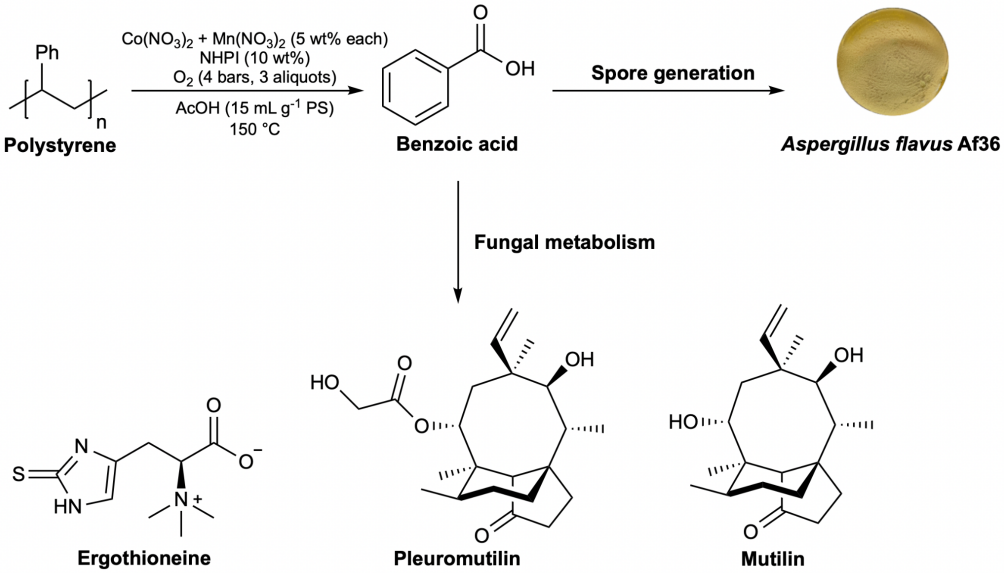

Scheme 1. Upcycling PS into structurally diverse SMs and spores of biocontrol agents. Post-consumer PS was collected and subjected to catalytic, oxidative cleavage to generate BA in high yield. This BA is then utilized as a sole carbon source by engineered strains of A. nidulans to generate the SMs ergothioneine, pleuromutilin, and mutilin. Furthermore, this BA is also used to generate high quantities of spores of the atoxigenic biocontrol agent *A. flavus* Af36.Importantly, current approaches to biologically upcycle PS deliver simple, low-value compounds; thus, methods that fully exploit fungal biosynthesis rapidly to upcycle PS have potential to create disproportionate value in our portfolio of polymer recyclates.

We recently reported an oxidative catalytic method rapidly to degrade post-consumer polyethylenes into distributions of carboxylic diacids.[32] Diacids suitable for fungal metabolism are then upgraded by engineered strains of fungi to high quantities of pharmacologically active secondary metabolites (SMs), all in under one week. Inspired by reports that fungi can utilize BA as a carbon source,[33-35] we hypothesized that the same oxidative chemistry used to degrade polyethylenes can likewise be applied to PS to generate BA or oligomers suitable for digestion. If confirmed, this would represent a major step toward our ability to upcycle mixed plastics.

As such, we collected post-consumer PS, including ocean waste sourced from Catalina Harbor on Santa Catalina Island, CA and subjected it to degradation. By employing similar oxidative conditions, we demonstrate that our catalytic system can be used to convert PS sourced from post-consumer and oceanic waste streams to BA (illustrated by ^{1}H NMR, Fig. S1) with up to 71% molar yield in 12 hours. While pristine BA can be isolated from this method, we collected crude product containing oligomeric material, thus enabling collection of > 71% of this PS material. This combined fraction was then used for fungal upgrading.

Having demonstrated that we can generate BA from PS, we then implemented genetic engineering techniques to promote SM biosynthesis. Fungi are ideal candidates for plastic upgrading due to their rapid growth, robust biosynthetic capabilities, genetic tractability, inexpensive cultivation requirements, and high fermentation titers. Collectively, these characteristics confer the ability to produce diverse products worth billions of dollars annually.[36] Attributable to advances in genome sequencing, our understanding of fungal biosynthesis has rapidly progressed and facilitated the development of efficient and customizable fungal fermentation platforms.

We leveraged these advances to enable production of the structurally diverse and pharmacologically active fungal SMs ergothioneine, pleuromutilin, and mutilin from engineered strains of the filamentous fungus *Aspergillus nidulans* using PS-derived BA. By introducing exogenous genes encoding biosynthetic enzymes into an *A. nidulans* host and placing them under the inducible *alcA* promoter (*alcA*(p)), we generated strains capable of upgrading PS digestion products to useful quantities of these SMs in under one week. Finally, we use PS-derived BA to generate spores of the *A. flavus* Af36, an agriculturally relevant biocontrol agent used to mitigate levels of aflatoxin, a highly carcinogenic and mutagenic mycotoxin.

Our overall route to upgrade PS exploits crude digest, which is then converted to either medically relevant SMs or spores of a biocontrol agent (Scheme 1). Taken together, this approach enables upcycling of post-consumer PS into multiple high-value products.

RESULTS AND DISCUSSION

Catalytic PS Degradation Conditions

We initiated our investigation of conditions for PS degradation using styrofoam insulated boxes (Table S1) that we shredded by hand. We monitored BA generation via ^{1}H NMR integration as a readout for the optimization of our catalytic conditions (Fig. S1). Low conversion efficiencies were observed with manganese(II) acetoacetonate, while the corresponding nitrate salt afforded a more reactive cleavage system (entries 1-3). Interestingly, we found that the introduction of cobalt together with manganese synergistically promoted BA generation. For example, 5 wt% each of two

nitrate salts afforded a 26% yield of BA after four hours, but 10 wt% of either catalyst alone could not permit a comparable conversion (entries 3-5).

Under optimal conditions with portion-wise recharging of O_2, we observed the complete degradation of PS with up to 71% of starting material recovered as BA and 84% total mass recovery (entries 5-7). The added balance likely comprises incompletely digested oligomers. We also note that a reduction in reaction time did not afford increased product yield, even under optimized conditions (entries 8-10).

Based on literature analogy for the use of these conditions to cleave alkyl ketones[37] and on our experience with them in polyethylene cleavage[32], we propose that manganese can act as a Lewis acid, coordinating intermediate polymer oxygenates. This seems to facilitate the role of cobalt to catalyze the β-scission for C-C bond cleavage, although the details of how these conditions engage PS are not yet fully elucidated.

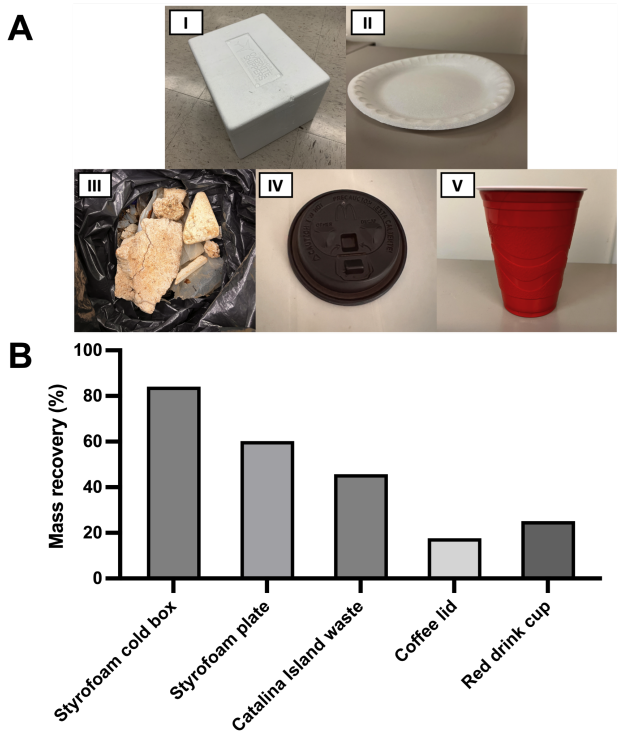

Figure 1. (A) Post-consumer PS sources used in this study; (B) Mass recoveries corresponding to each PS source. (I) Styrofoam cold box; (II) Styrofoam plate; (III) Catalina Island waste; (IV) Coffee lid; (V) Red drink cup.

We tested our conditions on four additional post-consumer PS sources: a styrofoam plate, waste collected from Santa Catalina Island, CA, a disposable coffee cup lid, and a red drink cup (Fig. 1). The styrofoam plate and Catalina Island waste (Table S2, entries 2-3) were efficiently homogenized into BA, with 51 and 39% molar yield, respectively. The coffee lid and red drink cup (entries 4-5) were also degraded into BA, with 15 and 21% molar yield, respectively. The differences in recoveries can be explained by the presence of additives, such as free radical scavengers and composite polymers, that may inhibit catalytic oxidation. Trash was collected specifically from Catalina Harbor because the Harbor's unique geography accumulates pieces of the Great Pacific Garbage Patch that wash up from the North Pacific Gyre. This enables us to demonstrate our method as an approach to recycle the Garbage Patch itself.

Following catalysis optimization, we developed a simple procedure to isolate polymer digest for downstream fungal upgrading. A series of liquid-liquid extractions followed by recrystallization afforded BA in high purity as indicated by ^{1}H NMR (Fig. S2). For a detailed extraction protocol, see Materials & Methods.

Fungal Metabolism of BA

We first confirmed that fungi can utilize BA as a sole carbon source using the model filamentous fungus *A. nidulans* FGSC A4 (Fig. S3). We observed a slight discoloration in the presence of BA relative to glucose minimal media (GMM) positive controls, indicating some degree of BA-induced toxicity. We separately determined that BA was not significantly toxic to the fungus. We repeated the above experiments with phthalic acid, the hydrolysis product of the NHPI catalyst, to confirm that it is both unable to be metabolized and is nontoxic to the fungus (Fig. S3).

For initial metabolomics experiments, we utilized the strain *A. nidulans* LO10050 to determine if SMs can be generated from a BA standard as a carbon source. Reported previously,[32] LO10050 has been engineered to express certain genes from the asperfuranone biosynthetic gene cluster (BGC). The incorporation of a positive feedback promoter system into this strain drives production of the biosynthetic intermediate asperbenzaldehyde to very high levels. The high production yield of asperbenzaldehyde allowed us to easily compare initial culture conditions permissive of SM production from BA.

We took advantage of this robust asperbenzaldehyde production system to determine preliminary culture conditions for fungal metabolism of PS-derived BA. We noticed that incubation of fungal strains in the presence of a BA standard affected the morphology of the strain; spherical mycelia characteristic of filamentous fungi cultured in shake flasks were not observed in these culture conditions. Nevertheless, microscopic examination of culture medium revealed the presence of extensive hyphae, revealing that growth attributable to BA was still occurring. We therefore chose to use asperbenzaldehyde production as a surrogate endpoint for fungal growth during these initial experiments.

Due to its reported toxicity to fungi,[35] we next determined the concentration of a BA standard that permitted the highest yield of asperbenzaldehyde in liquid cultures. We found that LO10050 could dose-dependently utilize BA as a sole carbon source to generate asperbenzaldehyde (Fig. S4): production plateaued when LO10050 was cultured in MM supplemented with 12.5 g L^{-1} BA, with areas under the curve (AUCs) reaching ca. 270% that of GMM controls. We eventually observed a decrease in asperbenzaldehyde yield when cultures were supplemented with 15.0 g L^{-1} BA, presumably due to BA toxicity.

Finally, we noted several minor products from the PS digestion reaction apart from BA as detected by HPLC-DAD-MS (Fig. S5). To determine whether these products are likewise suitable for fungal metabolism, we monitored their

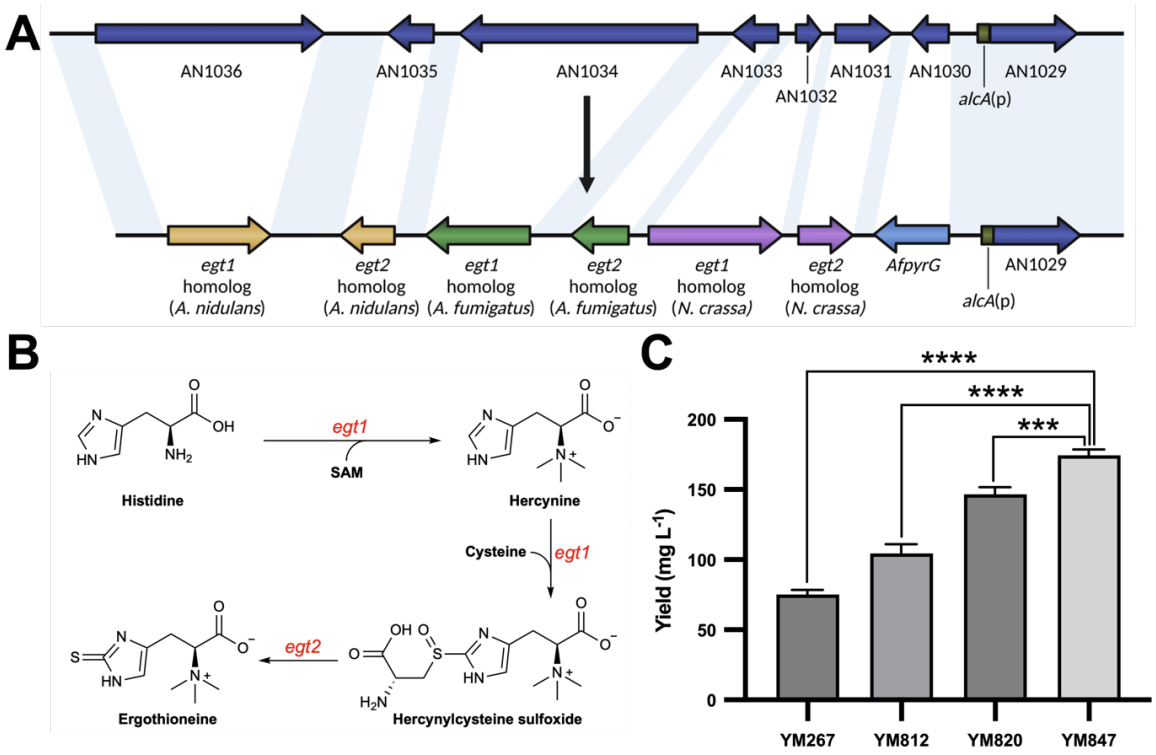

Figure 2. Strategy to enable heterologous ergothioneine production in *A. nidulans*. (A) Top: genetic architecture of the native *afo* regulon in *A. nidulans*. AN1029 (*afoA*) encodes a TF that regulates expression of each gene in the BGC, leading to production of asperfuranone, the final product of the pathway. Bottom: replacement of the coding regions of various genes in the *afo* regulon with endogenous (AN7620 and AN6227 from *A. nidulans*) and exogenous (Afu2g15650 and Afu2g13295 from *A. fumigatus*, NCU04343 and NCU11365 from *N. crassa*) ergothioneine biosynthetic genes. Expression of AfoA is driven to high levels by *alcA*(p), which then binds to the native promoter regions of genes within the *afo* regulon, leading to their expression. The *egt1* and *egt2* genes from *A. nidulans*, *A. fumigatus*, and *N. crassa* are shown in gold, green, and purple, respectively; (B) the biosynthetic pathway of ergothioneine in *N. crassa*; (C) relative ergothioneine yields from strains YM267, YM812, YM820, and YM847. Bars represent means and error bars represent SDs. **** $p \leq 0.0001$; *** $p \leq 0.0005$.

levels, along with asperbenzaldehyde and BA, in PSMM inoculated with LO10050 via HPLC-DAD-MS (Fig. S6). As expected, AUCs corresponding to asperbenzaldehyde increased and eventually plateaued after three days of incubation. BA AUCs closely mirrored those of asperbenzaldehyde; they gradually decreased over approximately three days. Lastly, AUCs corresponding to various minor products of PS digestion remained constant over the six-day incubation period, suggesting that BA is the only product of the digestion that is suitable for fungal metabolism.

Strain engineering – ergothioneine

To promote the efficient bioconversion of PS-derived BA in high yield, several genetic engineering strategies were employed to generate three medically and industrially relevant SMs: ergothioneine, pleuromutilin, and mutilin. The first SM that we aimed to generate from BA was ergothioneine, an unusual thio-histidine betaine amino acid.[38] Ergothioneine is a natural antioxidant that can be synthesized by certain species of fungi and actinobacteria. It has been reported to exhibit anti-inflammatory and cytoprotective properties, leading to its growing application in the pharmaceutical and cosmetic industries.[39]

Although discovered more than a century ago, there has recently been exponential growth in publications related to ergothioneine.[40] The genetic basis of its biosynthesis has been elucidated both in fungi and actinobacteria. In the latter, five genes (*egtABCDE*) direct its biosynthesis from histidine and cysteine.[41] However, fungi can synthesize ergothioneine using only two genes: *egt1* and *egt2* (Fig. 2).[42,43] To engineer a strain to produce ergothioneine in useful quantities, we took advantage of the robust *A. nidulans afo* regulon[44] to express ergothioneine biosynthetic genes. This regulon natively governs production of the polyketide SM asperfuranone; overexpression of *afoA*, encoding a cluster-specific transcription factor, has been shown strongly to activate all genes within the BGC, leading to production of very high levels of products of the cluster. To exploit the robust expression profile of this regulon, we replaced the coding regions of genes within the BGC with genes involved in ergothioneine biosynthesis.

First, BLASTp was used to identify putative *A. nidulans* homologs using the *Neurospora crassa egt1* and *egt2* as queries. This recovered two sequences bearing moderate homology to *egt1* and *egt2*: AN7620 (63% similarity/50% identity) and AN6227 (58% similarity/43% identity). AN7620 and AN6227 were then amplified using *A. nidulans* genomic DNA and inserted into the coding regions of *afoG* and *afoF*, respectively. Maintenance of the native promoters

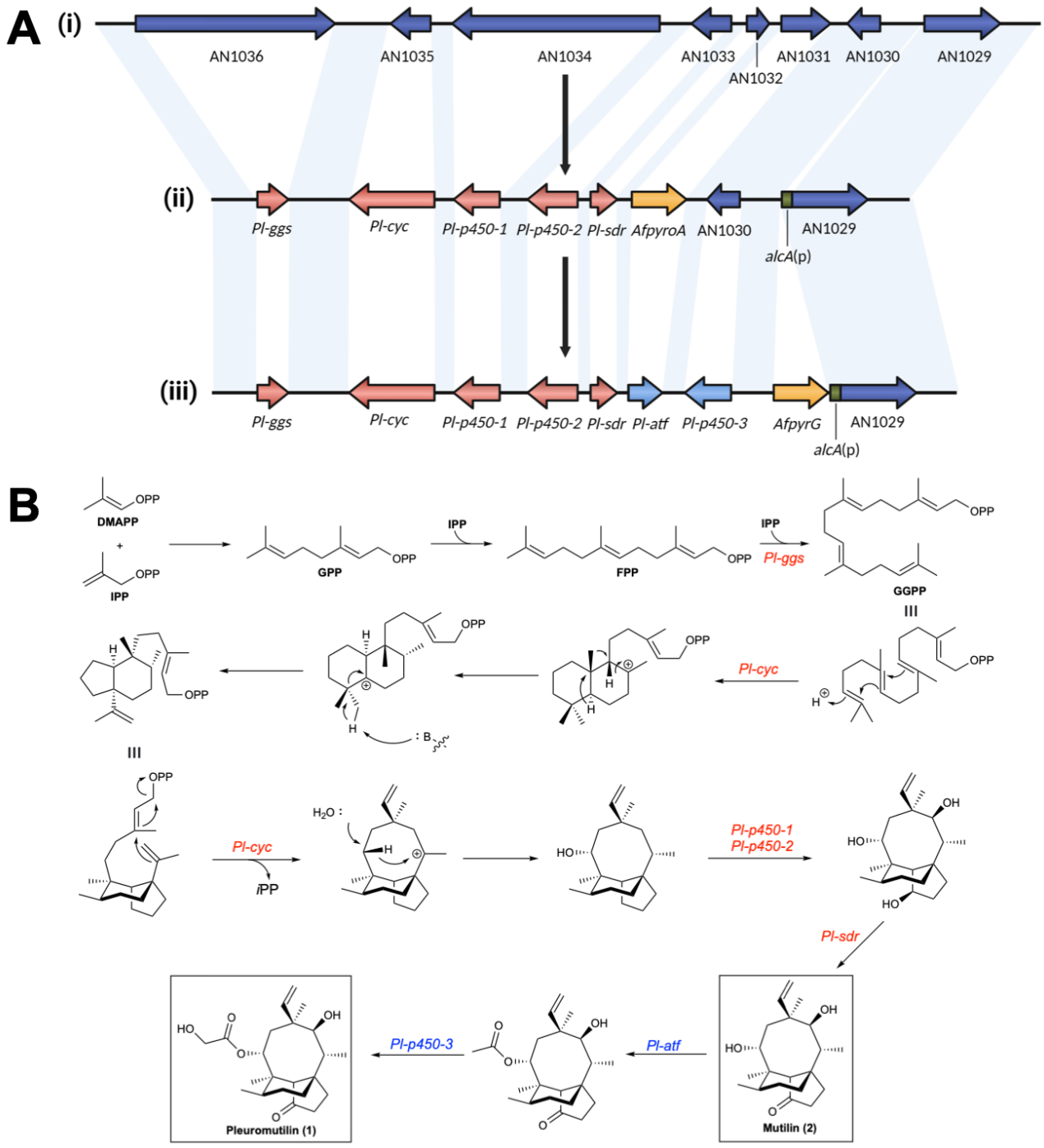

Figure 3. Strategy to enable heterologous mutilin and pleuromutilin production in *A. nidulans*. (A) Top: genetic architecture of the native *afo* regulon in *A. nidulans*. Middle: replacement of the coding regions of various genes in the *afo* regulon with exogenous mutilin biosynthetic genes. Expression of AfoA is driven to high levels by *alcA*(p), which then binds to the native promoter regions of genes within the *afo* regulon, leading to their expression. In total, five genes (orange) from *C. passeckerianus* were incorporated into the *afo* regulon to enable mutilin biosynthesis. Bottom: heterologous expression of two additional genes (gold) from *C. passeckerianus* into the *afo* regulon enables total reconstitution of the pleuromutilin biosynthetic pathway; (B) the biosynthetic pathway of mutilin and pleuromutilin. Dimethylallyl pyrophosphate (DMAPP) and isopentenyl pyrophosphate (IPP) first condense head-to-tail to form geranyl pyrophosphate (GPP). An additional IPP subunit condenses with GPP to form farnesyl pyrophosphate (FPP). Geranylgeranyl pyrophosphate synthase (*Pl-ggs*) condenses a final IPP subunit to form geranylgeranyl pyrophosphate (GGPP). GGPP undergoes intramolecular cyclization catalyzed by the gene product of *Pl-cyc* encoding a terpene cyclase. Two cytochrome p450s encoded by *Pl-p450-1* and *Pl-p450-2* catalyze the installation of two hydroxyl groups. The hydroxyl group bound to the cyclopentane ring is then oxidized to a ketone by the gene product of *Pl-sdr*, encoding a short-chain dehydrogenase/reductase, to form mutilin. An additional hydroxyl group bound to the cyclooctane ring is acetylated by the acetyltransferase encoded by *Pl-atf*. Finally, a cytochrome P450 encoded by *Pl-p450-3* hydroxylates the primary carbon within the acetyl group to yield pleuromutilin, the final product of the pathway.

of each of these genes allows for *afoA* to bind to them and drive their expression. We additionally replaced the native promoter of *afoA* with *alcA*(p) to create strain YM267.

To further increase yields, we replaced the coding regions of *afoE* and *afoD* with the *A. fumigatus egt1* (Afu2g15650) and *egt2* (Afu2g13295) homologs, respectively, to yield strain YM812. We inserted a third pair of ergothioneine biosynthetic genes into the regulon by replacing the coding regions of *afoC* and *afoB* with the *N. crassa egt1* (NCU04343) and *egt2* (NCU11365) to yield strain YM820.

Finally, we deleted the *agsB* gene encoding an α-1,3-glucan synthase[45] to create strain YM847. Deletion of genes encoding α-1,3-glucan synthases have been shown to improve fermentation titers by reducing hyphal clumping when grown in liquid cultures.[46] Collectively, these genetic engineering strategies enabled the generation of a strain expressing an inducible system controlling three pairs of ergothioneine biosynthetic genes (Fig. 2). The full biosynthetic pathway for ergothioneine in *N. crassa* is shown in Fig. 2B. All strains described above were cultured in triplicate to determine their relative ergothioneine titers. Gratifyingly, YM847 was able to produce over 170 mg L^{-1} ergothioneine and was therefore selected for subsequent upgrading of PS-derived BA.

Strain engineering – pleuromutilin and mutilin

We next utilized strains of *A. nidulans* engineered to synthesize the SMs pleuromutilin and mutilin from BA. Pleuromutilin, a diterpene natural product produced by the basidiomycete *Clitopilus passeckerianus*, was first discovered in 1950[47]. It and its derivatives function by selectively inhibiting bacterial translation by binding to the peptidyl transferase center of the bacterial ribosome.[48,49] Recently, the semisynthetic pleuromutilin derivative lefamulin was approved by the FDA for the treatment of community-acquired bacterial pneumonia.[50] Its biosynthetic pathway, involving seven genes in total, was recently elucidated.[51,52]

We utilized strain YM343, reported recently by our group,[53] that was engineered to reconstitute the entire pleuromutilin biosynthetic pathway to produce pleuromutilin from PS-derived BA. Each gene of interest was placed under control of the *afo* regulon to drive expression to very high levels. We also utilized strain YM283, which expresses only five of the seven genes within the pleuromutilin BGC, to produce its precursor, mutilin. Production of a biosynthetic precursor of the final product in the pathway should enable late-stage synthetic derivatization. Details regarding the biosynthetic pathway of mutilin and pleuromutilin are shown in Fig. 3.

Comparative metabolomics

We next determined if engineered fungal strains can biosynthesize SMs from PS-derived BA. Metabolic profiling of strains YM847, YM343, and YM283 revealed that all three metabolites can be produced in useful quantities from engineered strains of *A. nidulans* when grown in minimal media supplemented with PS-derived BA (PSMM) as a carbon source (Fig. 4). To quantify SM yields, standard curves for each SM were generated via HPLC-DAD or HPLC-DAD-MS (Figs. S7-9). Further, we isolated each of these SMs from and confirmed their structures and formulae via ^{1}H and ^{13}C NMR (Figs. S10-15 and Tables S3-8) and high-resolution mass spectrometry (Table S9). We note that, although SM yields in GMM are higher than in PSMM, the generation of non-trivial quantities of these valuable SMs from post-consumer PS still represents a transformative approach to PS upcycling. We further note that these strains were able to produce these SMs with minimal optimization in shake flasks. Optimization studies along with alteration of culture parameters should easily enable higher SM yields.

Biocontrol agent spore generation

Finally, we sought to determine if spores of an agriculturally relevant biocontrol agent can be generated from PS-derived BA. This is of particular importance to the field of plastics upcycling, because the biocatalytic products produced to date, while more valuable than the parent polymer, are not frequently used on scales that approach the quantity of plastic that will ultimately need to be reclaimed. Thus, it is valuable to add widely used agrichemicals to our product portfolio.

To demonstrate this, we generated spores of *A. flavus* Af36, a strain that is currently approved for use in the United States by the Environmental Protection Agency as a biocontrol agent for aflatoxin accumulation in peanuts, maize, and cottonseed.[54] Most strains of *A. flavus* are opportunistic pathogens that frequently infect maize, peanuts, cottonseed, and tree nuts.[55] These strains produce a family of highly carcinogenic and mutagenic polyketide-derived SMs termed aflatoxins. Aflatoxins inflict massive crop losses and account for an estimated 28% of global cases of liver cancers. Roughly 4.5 billion people have been exposed to unsafe levels of aflatoxins.[56]

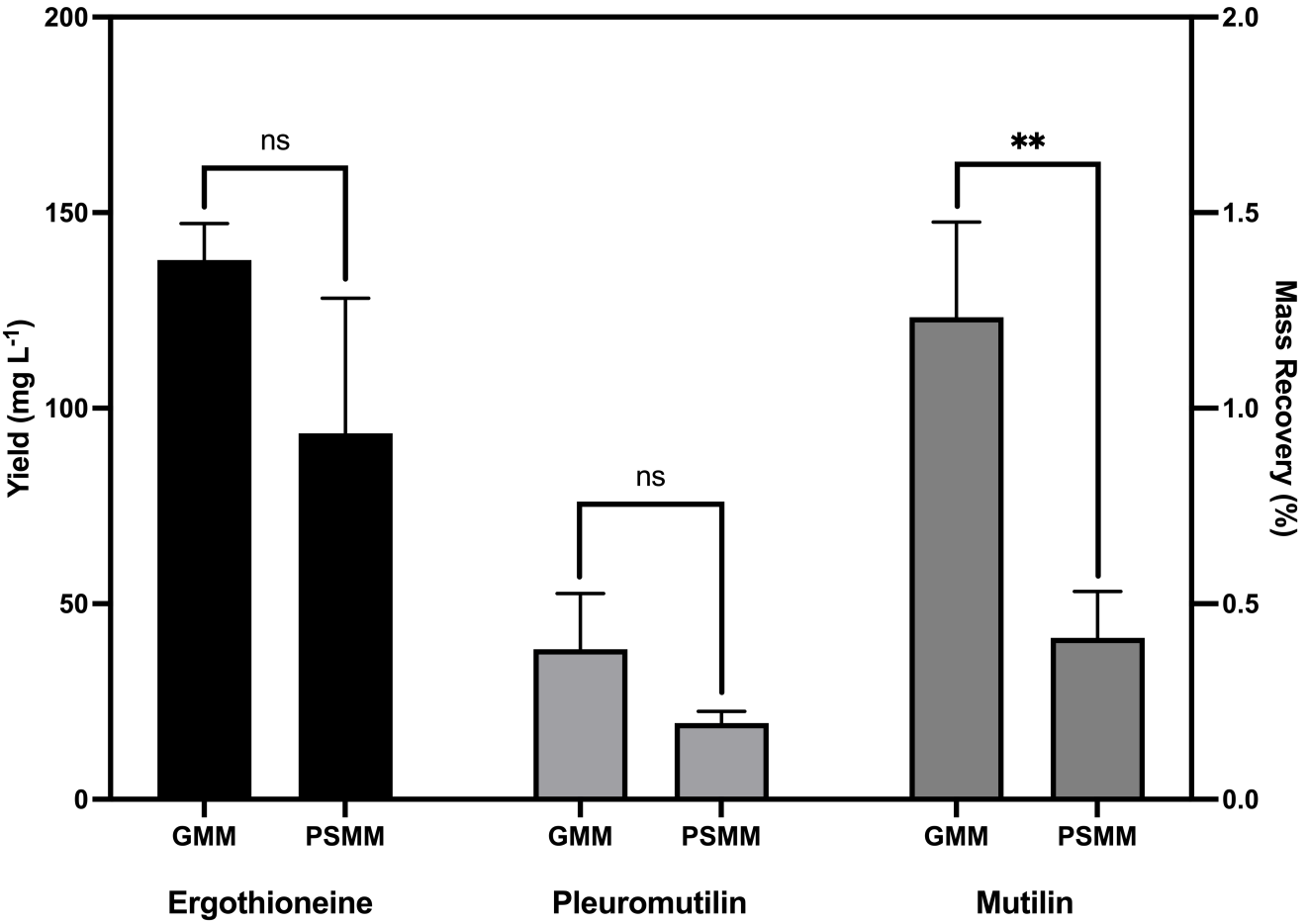

Figure 4. Comparative metabolomics of engineered strains of *A. nidulans* when cultured in GMM vs. PSMM. 1.0 x 10^7 spores of YM847, YM343, or YM283 were cultured in liquid GMM or PSMM. Relative SM levels were quantified using HPLC-DAD (for ergothioneine) or HPLC-DAD-MS (for pleuromutilin and mutilin). Bars represent means and error bars represent SDs. ns, not significant; ** $p \leq 0.01$.

Accordingly, many academic, industrial, and government groups have focused on mitigating risks of aflatoxins over the preceding decades. One such method is through the use of *A. flavus* strain Af36. This natural strain, first isolated from Arizona, lacks the ability to produce aflatoxin due to a single nucleotide polymorphism in the polyketide synthase *aflC* within the aflatoxin biosynthetic gene cluster (BGC).[57-59] *A. flavus* Af36 can competitively displace aflatoxin-producing strains of *A. flavus*, thereby limiting aflatoxin exposure. The generation of spores of this strain directly from PS-derived BA represents a unique and sustainable application of PS upcycling that has potential mass demand that could address a meaningful portion of PS waste.

To determine the feasibility of this application, we cultured *A. flavus* Af36 on solid GMM, MM, and PSMM agar plates and quantified spore generation after a seven-day incubation period. Our results indicate that spores of *A. flavus* Af36 can readily be generated using PS-derived BA (Fig. 5), with yields being 5.2-fold higher in PSMM relative to GMM.

CONCLUSIONS

Building out a robust and diversified portfolio of methods to reclaim value embedded in waste plastics, including PS, remains an evergreen challenge. Here, we couple catalytic oxidation with genetic engineering to develop a route to convert PS to fungal SMs within one week. In principle, any SM for which the biosynthetic pathway has been elucidated should be able to be generated from these PS-derived substrates, provided a robust expression system is established. We also demonstrate that we can generate spores of the agriculturally relevant biocontrol agent *A. flavus* Af36 from this PS-derived substrate. This adds important depth to the biocatalytic plastics upcycling portfolio because it shows a route that would consume upcycled plastics on an agrichemical scale.

Further, the enzymatic nature of biosynthesis coupled with high SM yields described here and previously[32] also implies high protein levels. Thus, this approach should also enable the production of proteins themselves from these plastic-derived substrates. Lastly, the production of other fungal fermentation products, such as organic acids, dyes, biofuels, and biopolymers should be available by these same methods. Thus, this platform effectively expands the catalog

of products derived from PS from relatively few, structurally simple compounds to, in principle, thousands of natural products. This work provides a path to apply material up-cycled from ocean-sourced waste to the promotion of human health and protection of the global food supply.

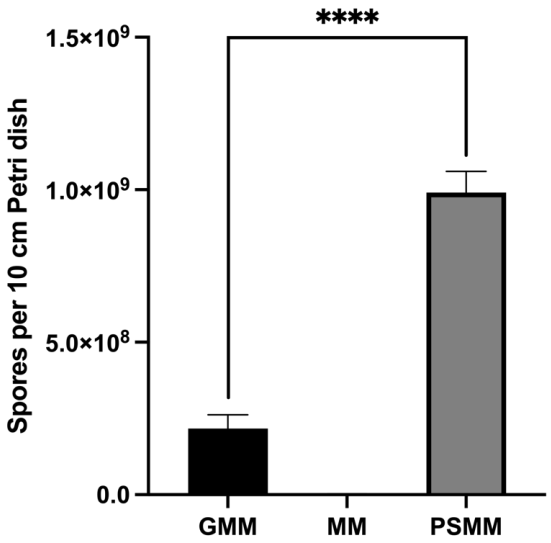

Figure 5. The generation of spores of *A. flavus* Af36 from PS-derived BA. *A. flavus* Af36 is an atoxigenic strain that lacks the ability to produce aflatoxins. It is currently used agriculturally by inoculation onto crops at various stages of their development. Following inoculation, it outcompetes toxigenic strains of *A. flavus*, thereby mitigating aflatoxin levels. Bars represent means and error bars represent SD. **** $p < 0.0001$.

ASSOCIATED CONTENT

Supporting Information

The Supporting Information is available free of charge on the ACS Publications website.

Procedures for catalyst screening, condition optimization, digest purification, media & buffer recipes, culture conditions, strain construction, SM extraction & quantification, compound purification & characterization, NMR spectra and chemical shift data, culturing results, and SM standard curves (PDF).

AUTHOR INFORMATION

Corresponding Authors

*Travis J. Williams, travisw@usc.edu
*Clay C. C. Wang, clayw@usc.edu

Author Contributions

The manuscript was written through contributions of all authors. #These authors contributed equally.

Funding Sources

This study was funded by the National Science Foundation (CHE-1856395); the National Institute of Health (R21-AI156320); the Department of Energy (Pacific Northwest National Laboratories subcontract); the University of Southern California (Dornsife College faculty working group, and Zumberge fund); the University of Southern California Wrigley Institute for Environmental Studies (Innovation award) and the University of Kansas Endowment (Irving S. Johnson Fund). Any funds used to support the research of the manuscript should be placed here (per journal style).

ACKNOWLEDGMENT

We are grateful to Dr. Nancy Keller for providing *A. flavus* Af36 and to Dr. Jason Stajich for providing *N. crassa*. We also thank Maria Tangalos and Salma Durra for assistance in fungal culturing experiments, Megan Fisk and Katie Macfee for assistance with chemical synthesis, and Dr. Robert Currier (Los Alamos National Laboratory) for helpful discussion regarding reactor experimental design. We further thank Conner Cheng Fong Wang, Jennifer Shyong, Celis Lee, Michael de Guzman, Nathan Vipapan, Jiayue Abby Geng, Brandon Wong, Alexa Cueva, and Ethan Hamid for their assistance in collecting post-consumer plastics from Santa Catalina Island, CA. We also thank the Boy Scouts of America for ocean plastics cleanup efforts.

ABBREVIATIONS

PS, polystyrene; EPS, expanded polystyrene foam; BA, benzoic acid; PHA, polyhydroxyalkanoates; SM, secondary metabolites; NMR, nuclear magnetic resonance; *alcA*(p), *alcA* promoter; GMM, glucose minimal medial; MM, minimal media; PSMM, polystyrene minimal media; NHPI, *N*-hydroxyphthalimide; BGC, biosynthetic gene cluster; FDA, Food and Drug Administration; IPP; isopentenyl pyrophosphate; DMAPP, dimethylallyl pyrophosphate; GPP, geranyl pyrophosphate; FPP, farnesyl pyrophosphate; GGPP, geranylgeranyl pyrophosphate; P450, cytochrome P450 monooxidase; HPLC-DAD, high-performance liquid chromatography; HPLC-DAD-MS, high-performance liquid chromatography-mass spectrometry; PCR, polymerase chain reaction; DNA, deoxyribonucleic acid; $NaNO_3$, sodium nitrate; KH_2PO_4, Monopotassium phosphate; KCl, potassium chloride; $MgSO_4 \cdot 7H_2O$, magnesium sulfate heptahydrate; KOH, potassium hydroxide; DCM, dichloromethane; MeOH, methanol; DMSO, dimethylsulfoxide; AcN, acetonitrile; EA, ethyl acetate.

REFERENCES

1. *Advancing Sustainable Materials Management: 2018 Tables and Figures* (pp. 1–80). (2020). United States Environmental Protection Agency.
2. Wünsch, J. R. (2000). *Polystyrene: Synthesis, Characteristics and Applications* (Vol. 10, p. 5). Shropshire: iSmithers Rapra Publishing.
3. Rahimi, A., & García, J. M. (2017). Chemical recycling of waste plastics for new materials production. *Nature Reviews Chemistry*, *1*(6), 0046. https://doi.org/10.1038/s41570-017-0046
4. Ho, B. T., Roberts, T. K., & Lucas, S. (2018). An overview on biodegradation of polystyrene and modified polystyrene: The microbial approach. *Critical Reviews in Biotechnology*, *38*(2), 308–320. https://doi.org/10.1080/07388551.2017.1355293
5. Kim, H. R., Lee, H. M., Yu, H. C., Jeon, E., Lee, S., Li, J., & Kim, D.-H. (2020). Biodegradation of Polystyrene by *Pseudomonas* sp. Isolated from the Gut of Superworms (Larvae of *Zophobas atratus*). *Environmental Science & Technology*, *54*(11), 6987–6996. https://doi.org/10.1021/acs.est.0c01495
6. Savoldelli, J., Tomback, D., & Savoldelli, H. (2017). Breaking down polystyrene through the application of a two-step thermal degradation and bacterial method to produce usable byproducts. *Waste Management*, *60*, 123–126. https://doi.org/10.1016/j.wasman.2016.04.017
7. Rochman, C. M., Manzano, C., Hentschel, B. T., Simonich, S. L. M., & Hoh, E. (2013). Polystyrene

Plastic: A Source and Sink for Polycyclic Aromatic Hydrocarbons in the Marine Environment. *Environmental Science & Technology*, *47*(24), 13976–13984. https://doi.org/10.1021/es403605f

8. Koelmans, A. A., Besseling, E., & Shim, W. J. (2015). Nanoplastics in the Aquatic Environment. Critical Review. In *Marine Anthropogenic Litter* (pp. 325–340). Springer International Publishing. https://doi.org/10.1007/978-3-319-16510-3_12
9. Huang, Z., Shanmugam, M., Liu, Z., Brookfield, A., Bennett, E. L., Guan, R., Vega Herrera, D. E., Lopez-Sanchez, J. A., Slater, A. G., McInnes, E. J. L., Qi, X., & Xiao, J. (2022). Chemical Recycling of Polystyrene to Valuable Chemicals via Selective Acid-Catalyzed Aerobic Oxidation under Visible Light. *Journal of the American Chemical Society*, *144*(14), 6532–6542. https://doi.org/10.1021/jacs.2c01410
10. Choi, D., Bang, J., Kim, T., Oh, Y., Hwang, Y., & Hong, J. (2020). In vitro chemical and physical toxicities of polystyrene microfragments in human-derived cells. *Journal of Hazardous Materials*, *400*, 123308. https://doi.org/10.1016/j.jhazmat.2020.123308
11. Wu, B., Wu, X., Liu, S., Wang, Z., & Chen, L. (2019). Size-dependent effects of polystyrene microplastics on cytotoxicity and efflux pump inhibition in human Caco-2 cells. *Chemosphere*, *221*, 333–341. https://doi.org/10.1016/j.chemosphere.2019.01.056
12. Hou, B., Wang, F., Liu, T., & Wang, Z. (2021). Reproductive toxicity of polystyrene microplastics: In vivo experimental study on testicular toxicity in mice. *Journal of Hazardous Materials*, *405*, 124028. https://doi.org/10.1016/j.jhazmat.2020.124028
13. Kik, K., Bukowska, B., & Sicińska, P. (2020). Polystyrene nanoparticles: Sources, occurrence in the environment, distribution in tissues, accumulation and toxicity to various organisms. *Environmental Pollution*, *262*, 114297. https://doi.org/10.1016/j.envpol.2020.114297
14. Paul-Pont, I., Lacroix, C., González Fernández, C., Hégaret, H., Lambert, C., Le Goïc, N., Frère, L., Cassone, A.-L., Sussarellu, R., Fabioux, C., Guyomarch, J., Albentosa, M., Huvet, A., & Soudant, P. (2016). Exposure of marine mussels Mytilus spp. To polystyrene microplastics: Toxicity and influence on fluoranthene bioaccumulation. *Environmental Pollution*, *216*, 724–737. https://doi.org/10.1016/j.envpol.2016.06.039
15. Lee, K.-W., Shim, W. J., Kwon, O. Y., & Kang, J.-H. (2013). Size-Dependent Effects of Micro Polystyrene Particles in the Marine Copepod *Tigriopus japonicus*. *Environmental Science & Technology*, *47*(19), 11278–11283. https://doi.org/10.1021/es401932b
16. Mensah, K., Mahmoud, H., Fujii, M., & Shokry, H. (2021). Upcycling of Polystyrene Waste Plastics to High Value Carbon by Thermal Decomposition. *Key Engineering Materials*, *897*, 103–108. https://doi.org/10.4028/www.scientific.net/KEM.897.103
17. Achilias, D. S., Kanellopoulou, I., Megalokonomos, P., Antonakou, E., & Lappas, A. A. (2007). Chemical Recycling of Polystyrene by Pyrolysis: Potential Use of the Liquid Product for the Reproduction of Polymer. *Macromolecular Materials and Engineering*, *292*(8), 923–934. https://doi.org/10.1002/mame.200700058
18. Oh, S., & Stache, E. E. (2022). Chemical Upcycling of Commercial Polystyrene via Catalyst-Controlled Photooxidation. *Journal of the American Chemical Society*, *144*(13), 5745–5749. https://doi.org/10.1021/jacs.2c01411
19. Huang, Z., Shanmugam, M., Liu, Z., Brookfield, A., Bennett, E. L., Guan, R., Vega Herrera, D. E., Lopez-Sanchez, J. A., Slater, A. G., McInnes, E. J. L., Qi, X., & Xiao, J. (2022). Chemical Recycling of Polystyrene to Valuable Chemicals via Selective Acid-Catalyzed Aerobic Oxidation under Visible Light. *Journal of the American Chemical Society*, *144*(14), 6532–6542. https://doi.org/10.1021/jacs.2c01410
20. Li, T., Vijeta, A., Casadevall, C., Gentleman, A. S., Euser, T., & Reisner, E. (2022). Bridging Plastic Recycling and Organic Catalysis: Photocatalytic Deconstruction of Polystyrene via a C–H Oxidation Pathway. *ACS Catalysis*, *12*(14), 8155–8163. https://doi.org/10.1021/acscatal.2c02292
21. Cao, R., Zhang, M.-Q., Hu, C., Xiao, D., Wang, M., & Ma, D. (2022). Catalytic oxidation of polystyrene to aromatic oxygenates over a graphitic carbon nitride catalyst. *Nature Communications*, *13*(1), 4809. https://doi.org/10.1038/s41467-022-32510-x
22. Motta, O., Proto, A., De Carlo, F., De Caro, F., Santoro, E., Brunetti, L., & Capunzo, M. (2009). Utilization of chemically oxidized polystyrene as co-substrate by filamentous fungi. *International Journal of Hygiene and Environmental Health*, *212*(1), 61–66. https://doi.org/10.1016/j.ijheh.2007.09.014
23. Milstein, O., Gersonde, R., Huttermann, A., Chen, M. J., & Meister, J. J. (1992). Fungal biodegradation of lignopolystyrene graft copolymers. *Applied and Environmental Microbiology*, *58*(10), 3225–3232. https://doi.org/10.1128/aem.58.10.3225-3232.1992
24. Galgali, P., Varma, A. J., Puntambekar, U. S., & Gokhale, D. V. (2002). Towards biodegradable polyolefins: Strategy of anchoring minute quantities of monosaccharides and disaccharides onto functionalized polystyrene, and their effect on facilitating polymer biodegradation. *Chemical Communications*, *23*, 2884–2885. https://doi.org/10.1039/b209254a
25. Oikawa, E., Linn, Khin Thida, Endo, Takeshi, Oikawa, Taneaki, Ishibachi, Yoshinobu. (2003). Isolation and Characterization of Polystyrene Degrading Microorganisms for Zero Emission Treatment of Expanded Polystyrene. *Environmental Engineering Research*, *40*, 373–379. https://doi.org/10.11532/PROES1992.40.373
26. Mor, R., & Sivan, A. (2008). Biofilm formation and partial biodegradation of polystyrene by the actinomycete *Rhodococcus ruber*. *Biodegradation*, *19*(6), 851–858. https://doi.org/10.1007/s10532-008-9188-0
27. Yang, Y., Yang, J., Wu, W.-M., Zhao, J., Song, Y., Gao, L., Yang, R., & Jiang, L. (2015). Biodegradation and Mineralization of Polystyrene by Plastic-Eating Mealworms: Part 1. Chemical and Physical Characterization and Isotopic Tests. *Environmental Science & Technology*, *49*(20), 12080–12086. https://doi.org/10.1021/acs.est.5b02661
28. Yang, Y., Yang, J., Wu, W.-M., Zhao, J., Song, Y., Gao, L., Yang, R., & Jiang, L. (2015). Biodegradation and Mineralization of Polystyrene by Plastic-Eating Mealworms: Part 2. Role of Gut Microorganisms. *Environmental Science & Technology*, *49*(20), 12087–12093. https://doi.org/10.1021/acs.est.5b02663
29. Ward, P. G., de Roo, G., & O'Connor, K. E. (2005). Accumulation of Polyhydroxyalkanoate from Styrene and Phenylacetic Acid by *Pseudomonas putida* CA-3. *Applied and Environmental Microbiology*, *71*(4), 2046–2052. https://doi.org/10.1128/AEM.71.4.2046-2052.2005
30. Tan, G.-Y. A., Chen, C.-L., Ge, L., Li, L., Tan, S. N., & Wang, J.-Y. (2015). Bioconversion of Styrene to Poly(hydroxyalkanoate) (PHA) by the New Bacterial Strain *Pseudomonas putida* NBUS12. *Microbes and Environments*, *30*(1), 76–85. https://doi.org/10.1264/jsme2.ME14138
31. Sullivan, K. P., Werner, A. Z., Ramirez, K. J., Ellis, L. D., Bussard, J. R., Black, B. A., Brandner, D. G., Bratti, F., Buss, B. L., Dong, X., Haugen, S. J., Ingraham, M.

A., Konev, M. O., Michener, W. E., Miscall, J., Pardo, I., Woodworth, S. P., Guss, A. M., Román-Leshkov, Y., … Beckham, G. T. (2022). Mixed plastics waste valorization through tandem chemical oxidation and biological funneling. *Science*, *378*(6616), 207–211. https://doi.org/10.1126/science.abo4626

32. Rabot, C., Chen, Y., Bijlani, S., Chiang, Y.-M., Oakley, C. E., Oakley, B. R., Williams, T. J., & Wang, C. C. C. (2022). Conversion of Polyethylenes into Fungal Secondary Metabolites. *Angewandte Chemie International Edition*, e202214609. https://doi.org/10.1002/anie.202214609
33. Boschloo, J. G., Paffen, A., Koot, T., van den Tweel, W. J. J., van Gorcom, R. F. M., Cordewener, J. H. G., & Bos, C. J. (1990). Genetic analysis of benzoate metabolism in *Aspergillus niger*. *Applied Microbiology and Biotechnology*, *34*(2), 225–228. https://doi.org/10.1007/BF00166785
34. Boschloo, J. G., Moonen, E., van Gorcom, R. F. M., Hermes, H. F. M., & Bos, C. J. (1991). Genetic analysis of *Aspergillus niger* mutants defective in benzoate-4-hydroxylase function. *Current Genetics*, *19*(4), 261–264. https://doi.org/10.1007/BF00355052
35. Lubbers, R. J. M., & de Vries, R. P. (2021). Production of Protocatechuic Acid from *p* -Hydroxyphenyl (H) Units and Related Aromatic Compounds Using an *Aspergillus niger* Cell Factory. *MBio*, *12*(3), e0039121. https://doi.org/10.1128/mBio.00391-21
36. Meyer, V., Andersen, M. R., Brakhage, A. A., Braus, G. H., Caddick, M. X., Cairns, T. C., de Vries, R. P., Haarmann, T., Hansen, K., Hertz-Fowler, C., Krappmann, S., Mortensen, U. H., Peñalva, M. A., Ram, A. F. J., & Head, R. M. (2016). Current challenges of research on filamentous fungi in relation to human welfare and a sustainable bio-economy: A white paper. *Fungal Biology and Biotechnology*, *3*(6), 1-17. https://doi.org/10.1186/s40694-016-0024-8
37. Minisci, F., Punta, C., & Recupero, F. (2006). Mechanisms of the aerobic oxidations catalyzed by *N*-hydroxyderivatives. *Journal of Molecular Catalysis A: Chemical*, *251*(1–2), 129–149. https://doi.org/10.1016/j.molcata.2006.02.011
38. Borodina, I., Kenny, L. C., McCarthy, C. M., Paramasivan, K., Pretorius, E., Roberts, T. J., van der Hoek, S. A., & Kell, D. B. (2020). The biology of ergothioneine, an antioxidant nutraceutical. *Nutrition Research Reviews*, *33*(2), 190–217. https://doi.org/10.1017/S0954422419000301
39. Cheah, I. K., & Halliwell, B. (2012). Ergothioneine; antioxidant potential, physiological function and role in disease. *Biochimica et Biophysica Acta (BBA) - Molecular Basis of Disease*, *1822*(5), 784–793. https://doi.org/10.1016/j.bbadis.2011.09.017
40. Cheah, I. K., & Halliwell, B. (2021). Ergothioneine, recent developments. *Redox Biology*, *42*, 101868. https://doi.org/10.1016/j.redox.2021.101868
41. Seebeck, F. P. (2010). In Vitro Reconstitution of Mycobacterial Ergothioneine Biosynthesis. *Journal of the American Chemical Society*, *132*(19), 6632–6633. https://doi.org/10.1021/ja101721e
42. Hu, W., Song, H., Sae Her, A., Bak, D. W., Naowarojna, N., Elliott, S. J., Qin, L., Chen, X., & Liu, P. (2014). Bioinformatic and Biochemical Characterizations of C–S Bond Formation and Cleavage Enzymes in the Fungus *Neurospora crassa* Ergothioneine Biosynthetic Pathway. *Organic Letters*, *16*(20), 5382–5385. https://doi.org/10.1021/ol502596z
43. Pluskal, T., Ueno, M., & Yanagida, M. (2014). Genetic and Metabolomic Dissection of the Ergothioneine and Selenoneine Biosynthetic Pathway in the Fission Yeast, *S. pombe*, and Construction of an Overproduction System. *PLoS ONE*, *9*(5), e97774. https://doi.org/10.1371/journal.pone.0097774
44. Chiang, Y.-M., Szewczyk, E., Davidson, A. D., Keller, N., Oakley, B. R., & Wang, C. C. C. (2009). A Gene Cluster Containing Two Fungal Polyketide Synthases Encodes the Biosynthetic Pathway for a Polyketide, Asperfuranone, in *Aspergillus nidulans*. *Journal of the American Chemical Society*, *131*(8), 2965–2970. https://doi.org/10.1021/ja8088185
45. Yoshimi, A., Sano, M., Inaba, A., Kokubun, Y., Fujioka, T., Mizutani, O., Hagiwara, D., Fujikawa, T., Nishimura, M., Yano, S., Kasahara, S., Shimizu, K., Yamaguchi, M., Kawakami, K., & Abe, K. (2013). Functional Analysis of the α-1,3-Glucan Synthase Genes *agsA* and *agsB* in *Aspergillus nidulans*: AgsB Is the Major α-1,3-Glucan Synthase in This Fungus. *PLoS ONE*, *8*(1), e54893. https://doi.org/10.1371/journal.pone.0054893
46. Miyazawa, K., Yoshimi, A., Zhang, S., Sano, M., Nakayama, M., Gomi, K., & Abe, K. (2016). Increased enzyme production under liquid culture conditions in the industrial fungus *Aspergillus oryzae* by disruption of the genes encoding cell wall α-1,3-glucan synthase. *Bioscience, Biotechnology, and Biochemistry*, *80*(9), 1853–1863. https://doi.org/10.1080/09168451.2016.1209968
47. Kavanagh, F., Hervey, A., & Robbins, W. J. (1951). Antibiotic Substances From Basidiomycetes. *Proceedings of the National Academy of Sciences*, *37*(9), 570–574. https://doi.org/10.1073/pnas.37.9.570
48. Novak, R., & Shlaes, D. M. (2010). The pleuromutilin antibiotics: A new class for human use. *Current Opinion in Investigational Drugs (London, England : 2000)*, *11*(2), 182–191.
49. Poulsen, S. M., Karlsson, M., Johansson, L. B., & Vester, B. (2008). The pleuromutilin drugs tiamulin and valnemulin bind to the RNA at the peptidyl transferase centre on the ribosome. *Molecular Microbiology*, *41*(5), 1091–1099. https://doi.org/10.1046/j.1365-2958.2001.02595.x
50. *FDA approves new antibiotic to treat community-acquired bacterial pneumonia*. (2019, August 19).
51. Alberti, F., Khairudin, K., Venegas, E. R., Davies, J. A., Hayes, P. M., Willis, C. L., Bailey, A. M., & Foster, G. D. (2017). Heterologous expression reveals the biosynthesis of the antibiotic pleuromutilin and generates bioactive semi-synthetic derivatives. *Nature Communications*, *8*(1), 1831. https://doi.org/10.1038/s41467-017-01659-1
52. Bailey, A. M., Alberti, F., Kilaru, S., Collins, C. M., de Mattos-Shipley, K., Hartley, A. J., Hayes, P., Griffin, A., Lazarus, C. M., Cox, R. J., Willis, C. L., O'Dwyer, K., Spence, D. W., & Foster, G. D. (2016). Identification and manipulation of the pleuromutilin gene cluster from Clitopilus passeckerianus for increased rapid antibiotic production. *Scientific Reports*, *6*(1), 25202. https://doi.org/10.1038/srep25202
53. Chiang, Y.-M., Lin, T.-S., Chang, S.-L., Ahn, G., & Wang, C. C. C. (2021). An *Aspergillus nidulans* Platform for the Complete Cluster Refactoring and Total Biosynthesis of Fungal Natural Products. *ACS Synthetic Biology*, *10*(1), 173–182. https://doi.org/10.1021/acssynbio.0c00536
54. Kausch, J. (2017). *Aspergillus flavus AF36 Prevail* (pp. 1–6).
55. Klich, M. A. (2007). *Aspergillus flavus*: The major producer of aflatoxin. *Molecular Plant Pathology*, *8*(6), 713–722. https://doi.org/10.1111/j.1364-3703.2007.00436.x
56. Williams, J. H., Phillips, T. D., Jolly, P. E., Stiles, J. K., Jolly, C. M., & Aggarwal, D. (2004). Human aflatoxicosis in developing countries: A review of

toxicology, exposure, potential health consequences, and interventions. *The American Journal of Clinical Nutrition*, *80*(5), 1106–1122. https://doi.org/10.1093/ajcn/80.5.1106

57. Cotty, P. J. (1989). Virulence and cultural characteristics of two Aspergillus flavus strains pathogenic on cotton. *Phytopathology*, *79*(7), 808–814. https://doi.org/10.1094/Phyto-79-808.
58. Chang, P.-K., Horn, B. W., & Dorner, J. W. (2005). Sequence breakpoints in the aflatoxin biosynthesis gene cluster and flanking regions in nonaflatoxigenic *Aspergillus flavus* isolates. *Fungal Genetics and Biology*, *42*(11), 914–923. https://doi.org/10.1016/j.fgb.2005.07.004
59. Ehrlich, K. C., & Cotty, P. J. (2004). An isolate of *Aspergillus flavus* used to reduce aflatoxin contamination in cottonseed has a defective polyketide synthase gene. *Applied Microbiology and Biotechnology*, *65*(4), 473–478. https://doi.org/10.1007/s00253-004-1670-y

Insert Table of Contents artwork here

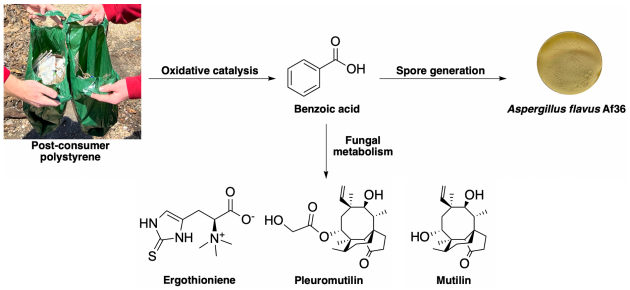

Supplementary Information

Polystyrene Upcycling into Fungal Natural Products and a Biocontrol Agent

Chris Rabot,[†#] Yuhao Chen,[‡§#] Shu-Yi Lin,[†] Ben Miller,[†‡] Yi-Ming Chiang,[†] C. Elizabeth Oakley,[‖] Berl R. Oakley,[‖] Clay C. C. Wang,[†‡§*] & Travis J. Williams[‡§*]

[†]Department of Pharmacology & Pharmaceutical Sciences, University of Southern California, 1985 Zonal Ave, Los Angeles, CA 90089.

[‡]Donald P. and Katherine B. Loker Hydrocarbon Institute and Department of Chemistry; 837 Bloom Walk, University of Southern California, Los Angeles, CA 90089.

[§]Wrigley Institute for Environmental Studies, 3454 Trousdale Parkway, Los Angeles, CA 90089.

[‖]Department of Molecular Biosciences, University of Kansas, 1200 Sunnyside Avenue, Lawrence, KS 66045.

[#]These authors contributed equally to this work.

*Corresponding authors. Emails: clayw@usc.edu, travisw@usc.edu

Materials & Methods

General methods

All commercially available chemicals were obtained from TCI America except for cobalt nitrate and manganese nitrate, which were purchased from Alfa Aesar, and BA, which was purchased from Sigma Aldrich. Acetic acid, hexane, and chloroform were obtained from EMD Millipore. The NMR solvents chloroform-*d* and methanol-d_4 were purchased from Cambridge Isotopes Laboratories. All solvents and metal salts were used as received, without any further purification.

All polystyrene (PS) waste including the styrofoam cold box, styrofoam plate, coffee lid, and red solo cup were collected from the waste stream. The mixed plastic waste samples were collected from Catalina Harbor at Santa Catalina Island, CA. All plastic waste samples were roughly cleaned with acetone, dried and then shredded using a benchtop coffee grinder before use.

^{1}H and ^{13}C NMR spectra were obtained by Varian VNMRS 600 or 400MR spectrometers and processed via MestreLab Mnova. All the chemical shifts are shown by the units of ppm and referenced to the residual ^{1}H solvent peak.

HPLC-DAD-MS spectra were acquired using a ThermoFinnigan LCQ Advantage ion trap mass spectrometer equipped with a reverse phase C_{18} column (Alltech Prevail C_{18}; particle size, 3 μm; column, 2.1 x 100 mm) with a flow rate of 125 μL min^{-1} . The solvents used were 95% AcN-H_2O (solvent B) in 5% AcN-H_2O (solvent A) plus 0.05% formic acid. The solvent gradient used was: 0% solvent B from 0 to 5 min, 0 to 100% solvent B from 5 to 35 min, 100% solvent B from 35 to 40 min, 100 to 0% solvent B from 40 to 45 min, and reequilibration with 0% solvent B from 45 to 50 min. MS conditions were as follows: 5.0 kV capillary voltage, sheath gas flow rate of 60 arbitrary units (AUs), auxiliary gas flow rate of 10 AUs, and ion transfer capillary temperature at 350 °C.

High-resolution mass spectra were acquired on a Thermo Fisher Q-Exactive Orbitrap mass spectrometer. MS conditions were as follows: _ kV capillary voltage, sheath gas flow rate of _ arbitrary units (AUs), auxiliary gas flow rate of _ AUs, and ion transfer capillary temperature at _ °C.

General procedure for catalyst screening

In a 300 mL Parr reactor, ground styrofoam PS powder (5 g) was mixed with NHPI (0.5 g), metal catalysts (0.5 g total) and acetic acid (75 mL). The reactor was then sealed and pressurized to four bars with molecular O_2 and stirred at 150 ^oC for four hours. The reactor was then cooled to room temperature and unsealed to release remaining O_2. Any volatiles, including acetic acid, were removed by rotary evaporation and the resulting product mixture was resuspended in 1 M NaOH (ca. 80-100 mL). Insoluble particles were removed by vacuum filtration. The resulting solution was acidified to pH 1 with concentrated HCl and extracted with ethyl acetate (EA) (3 x 150 mL). The combined organic fractions were dried over Na_2SO_4 and the solvent was removed by rotary evaporation to afford a dark yellow solid product mixture. The yield of BA was determined by ^1H NMR with 1,3,5-trimethoxybenzene as an internal standard.

Safety notes: all pressurized reactions should be isolated behind appropriately rated blast shields and conducted at the minimal requisite scale. All reactions involving pressurized oxygen gas must have appropriately specified burst disks. All operations involving heating acetic acid should be conducted in a chemical fume hood. An analysis of upper and lower flammability limits should be conducted before heating and combination of oxygen gas and organic solvent. No scaling of such procedures should be attempted without consulting appropriate experts in safety engineering[1].

General procedure for condition optimization

In a 300 mL Parr reactor, ground styrofoam PS powder (5 g) was mixed with cobalt nitrate (0.25 g), manganese nitrate (0.25 g), and acetic acid (75 mL). The reactor was pressurized with four bars O_2

and stirred at 150 °C for the specified period (see Table 1, entries 5-10). The reactor was then removed from the heat and cooled to room temperature (30 - 60 min). After recharging with O_2, the reactor was again heated to continue the reaction. After time periods specified in Table 1, the Parr reactor was cooled to room temperature and the internal pressure was released. The obtained crude mixture was processed using the same procedure described above to yield a dark yellowish solid mixture.

Digest purification

The obtained PS degradation mixture was resuspended in 50 mL chloroform in a 100 mL round-bottom flask, stirred (50 - 60 min) and then filtered. The chloroform was removed *in vacuo* to generate a light brown powder, which was washed with hot hexanes (ca. 50 °C, 3 x 50 mL) over a filter. The hexane extract was concentrated *in vacuo* to obtain a chalky powder.

To recrystallize BA, the hexane extract was dissolved in ca. 100 mL boiling water and passed through a fritted filter funnel. The flow-through was collected into a 250 mL Erlenmeyer flask placed in an ice bath and allowed to cool (60 min). The contents of the flask were passed through a clean filter funnel, and the obtained residue was flushed with ca. 100 mL cold water. The obtained residue was dried over a filter paper to yield a crystalline white powder.

Media & buffer recipes

All recipes are based on MM: 12.0 g L^{-1} $NaNO_3$, 3.04 g L^{-1} KH_2PO_4, 1.04 g L^{-1} KCl, 1.04 g L^{-1} $MgSO_4 \cdot 7H_2O$, and 1 mL L^{-1} Hutner's trace element solution[2]. GMM is MM supplemented with 10 g L^{-1} d-glucose. PSMM is MM supplemented with 10 g L^{-1} PS digest. Solid plates follow the same recipes as above with the addition of 15 g L^{-1} agar. All media were adjusted to pH 8.0 using 5.5 M KOH. ST buffer: 8.5 g L^{-1} NaCl, 1 mL L^{-1} Tween 80.

Asperbenzaldehyde production from BA

In order to confirm if fungal strains can utilize BA as a sole carbon source to generate SMs, ca. 3.0 x 10^7 spores of LO10050 were inoculated, in triplicate, into 125 mL Erlenmeyer flasks containing 30 mL MM supplemented with increasing concentrations (2.5, 5.0, 7.5, 10.0, 12.5, and 15.0 g L^{-1}) of a BA standard. Cultures were incubated for six days at 37 °C with shaking at 180 rpm. To lyse mycelia to release intracellular asperbenzaldehyde, 30 mL MeOH was added to each culture flask, which were sonicated for one hour. 10 µL aliquots of LO10050 extracts were then analyzed via HPLC-DAD-MS. Extracted ion chromatograms corresponding to asperbenzaldehyde were measured for each condition.

Fungal metabolism of PS digestion products

To determine if other products of the PS digestion reaction apart from BA are suitable for fungal metabolism, 3.0 x 10^7 spores of LO10050 were inoculated into a 125 mL Erlenmeyer flask containing 30 mL PSMM. Cultures were incubated for six days at 37 °C with shaking at 180 rpm. 200 µL aliquots of the culture medium were collected daily throughout a six-day incubation period. These aliquots were extracted with ca. 1 mL EA, dried, and resuspended in 200 µL 4:1 MeOH:DMSO. 10 µL of these extracts were then analyzed via HPLC-DAD-MS. Extracted ion chromatograms corresponding to each compound of interest were measured for each condition (Fig. S6).

Strain construction

All molecular genetic methods were carried out according to previously reported fusion PCR-based methods[3]. Briefly, genes of interest were amplified from genomic DNA and fused to promoters of interest, appropriate selectable markers, and flanking regions up- and downstream from target genomic loci. The resulting fusion PCR construct was transformed into fungal protoplasts, also generated according to previously reported methods[3].

SM extraction and quantification

For ergothioneine quantification, cultures of YM847 were heated in a 100 °C water bath for 20 minutes to lyse mycelia containing intracellular ergothioneine. 10 µL of this lysate was analyzed with HPLC-DAD without dilution. Extracts were analyzed with a Venusil HILIC column (4.6 x 250 mm, 5 µm). The solvent used was 4:1 AcN:20 mmol L^{-1} ammonium acetate (pH 6) at a flow rate of 1 mL min^{-1}.

For pleuromutilin and mutilin quantification, mycelia were filtered from the culture media and sonicated in 1:1 DCM:MeOH for one hour. The organic extracts were then filtered and dried (TurboVap LV). Once dried, extracts were resuspended in 20 mL ddH_2O and extracted three times with 20 mL EA. Organic extracts were then dried as above. Culture media (ca. 25 mL) were extracted three times with 25 mL EA. Organic extracts from the culture media were combined with those from the mycelia and dried. Extracts were resuspended in 10 mL 4:1 MeOH:DMSO and 10 µL of this extract was injected for HPLC-DAD-MS analysis.

Compound purification & characterization

For ergothioneine purification, ca. 1.0 x 10^7 spores of YM847 were inoculated into three 25 mL Erlenmeyer flasks, each containing 10 mL PSMM. Culture and induction parameters were the same as described above. To lyse mycelia, 10 mL MeOH was added to culture flasks, which were then sonicated for one hour. Culture media were then combined and filtered to remove fungal biomass. Culture media were concentrated *in vacuo* and subjected to reverse-phase column chromatography with gradient elution. The mobile phases used were 100% AcN followed by 9:1, 17:3, 4:1, and 7:3 AcN:ddH_2O. Fractions containing ergothioneine were combined, dried *in vacuo*, and subjected to final purification with reverse-phase preparative thin layer chromatography using 17:3 AcN:ddH_2O as a mobile phase. A band corresponding to ergothioneine was excised and flushed with ddH_2O over a fritted filter funnel. The aqueous extract was concentrated *in vacuo* to yield ergothioneine.

For pleuromutilin and mutilin purification, ca. 3.0 x 10^7 spores of YM343 and YM283, respectively, were inoculated into five 125 mL Erlenmeyer flasks, each containing 30 mL PSMM. Culture

and induction parameters were the same as described above. Following incubation, mycelia were filtered from the culture media. Culture media were extracted three times with 150 mL DCM and organic extracts were dried *in vacuo*. Extracts were then subject to purification by normal-phase column chromatography using the following mobile phase gradient: 9:1, 7:3, 1:1, 3:7, 1:9. Fractions containing pleuromutilin or mutilin were combined and subjected to final purification using normal-phase preparative thin layer chromatography (TLC). The mobile phases used were 1:1 for pleuromutilin and 3:7 EA:hexanes for mutilin. Bands corresponding to pleuromutilin or mutilin were excised and flushed with DCM over a fritted filter funnel. Organic extracts were concentrated *in vacuo* to yield pleuromutilin and mutilin.

Supplementary Figures

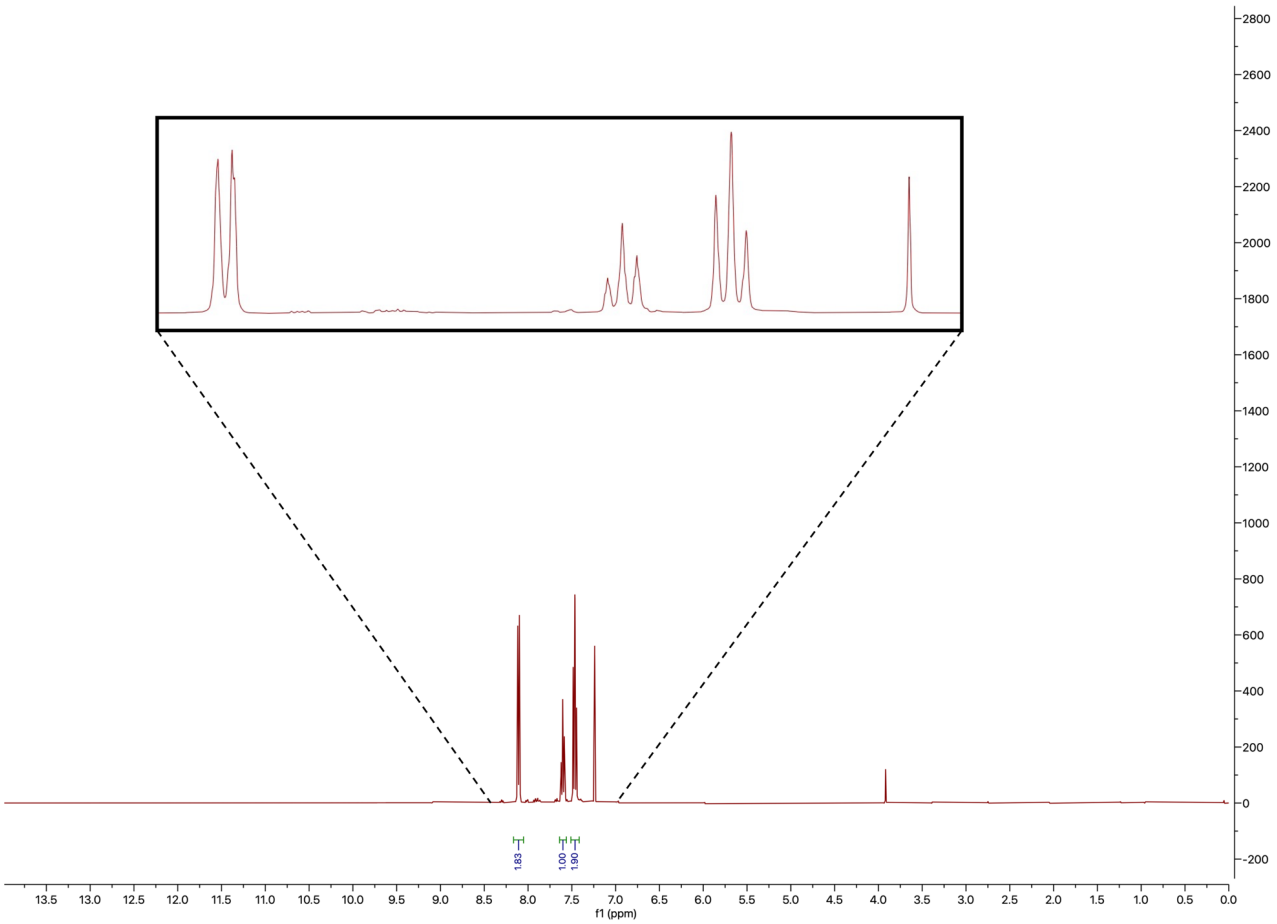

Figure S1. ^{1}H NMR spectrum of crude PS digest. The sample was dissolved in $CDCl_3$.

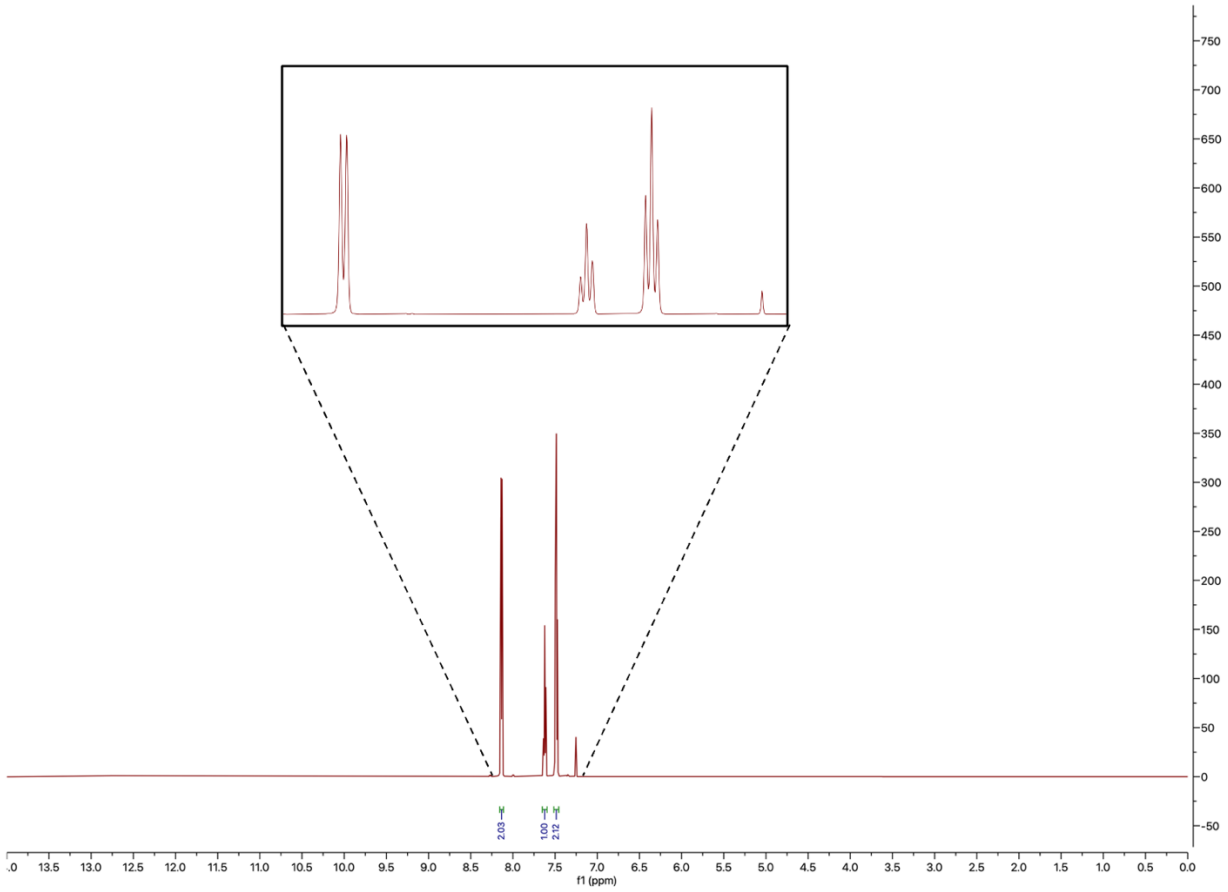

Figure S2. ^{1}H NMR spectrum of recrystallized BA derived from PS. The sample was dissolved in $CDCl_3$.

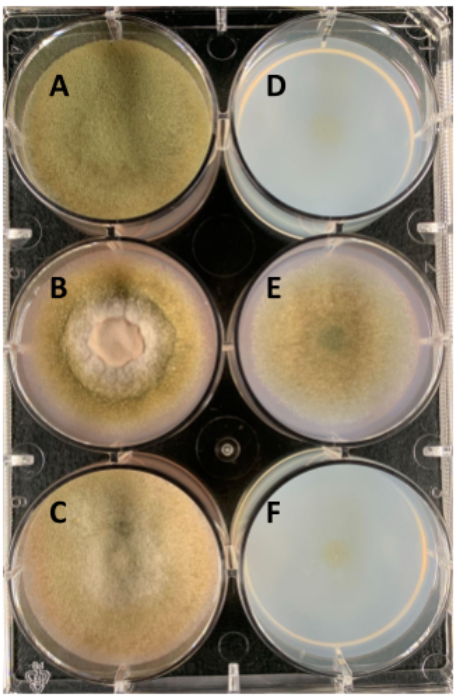

Figure S3. Fungal metabolism and toxicity of BA and phthalic acid. 1.0 x 10^6 spores of *A. nidulans* FGSC A4 were inoculated into 6-well plates containing 10 mL of (A) GMM, (B) GMM + 10 g L^{-1} BA, (C) GMM + 10 g L^{-1} phthalic acid, (D) MM, (E) MM + 10 g L^{-1} BA, (F) MM + 10 g L^{-1} phthalic acid. Cultures were incubated at 37 °C for seven days.

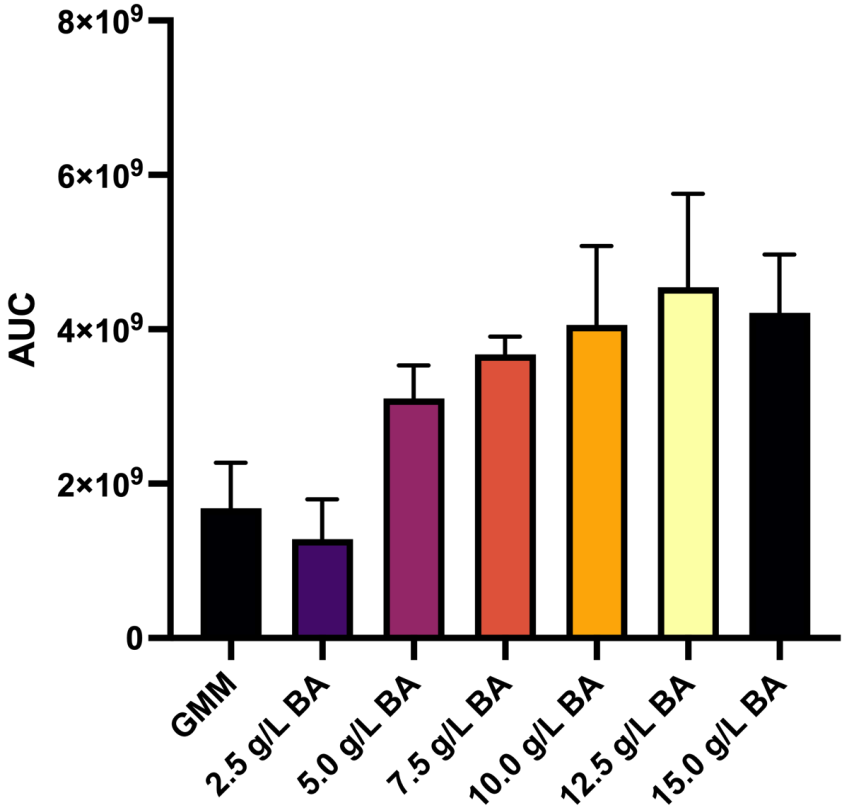

Figure S4. Asperbenzaldehyde production in GMM compared to MM supplemented with increasing concentrations of BA. 3.0 x 10^7 spores of LO10050 were inoculated into 125 mL Erlenmeyer flasks containing 30 mL of media. Each condition was cultured in triplicate. Cultures were incubated for six days at 37 °C with shaking at 180 rpm. Following incubation, 30 mL MeOH was added to each culture flask, which were then sonicated for one hour. 10 µL aliquots of extracts were then analyzed via HPLC-DAD-MS. Extracted ion chromatograms corresponding to asperbenzaldehyde were measured for each condition.

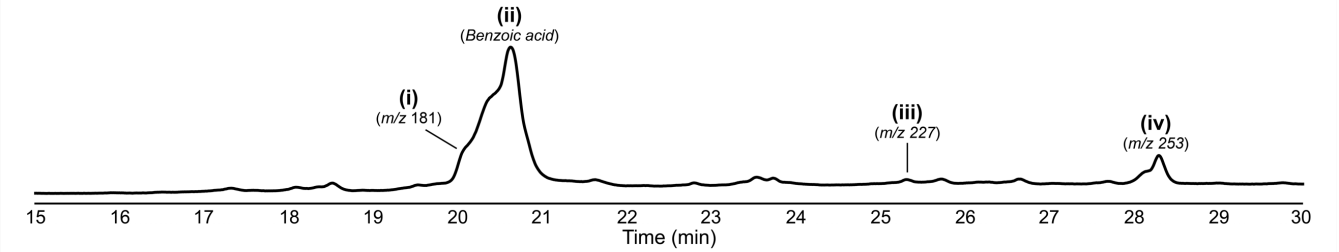

Figure S5. Representative total scan PDA chromatogram of crude PS digestion products generated via HPLC-DAD-MS. Positive-mode ESI *m/z* values and, when permissible, identities of compounds are annotated.

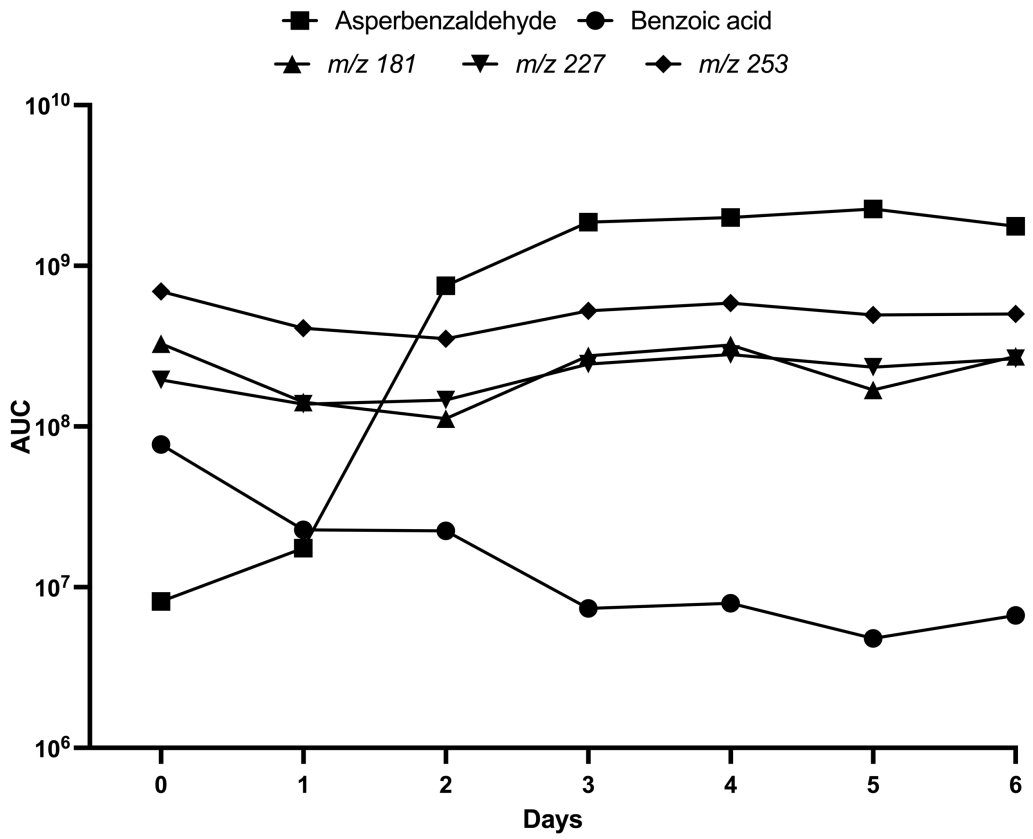

Figure S6. Fungal metabolism of PS digestion products and production of asperbenzaldehyde. 3.0 x 10^7 spores of LO10050 were inoculated into a 125 mL Erlenmeyer flask containing 30 mL of PSMM. Cultures were incubated at 37 °C with shaking at 180 rpm. 200 µL aliquots of culture media were collected daily for six days and extracted with 1 mL EA. Organic extracts were dried (TurboVap LV), resuspended in 200 µL 4:1 MeOH:DMSO, and analyzed via HPLC-DAD-MS. AUCs corresponding to benzoic acid, asperbenzaldehyde, and other minor PS digestion products (with *m/z* values in positive-mode ESI = 181, 227, and 253) were measured.

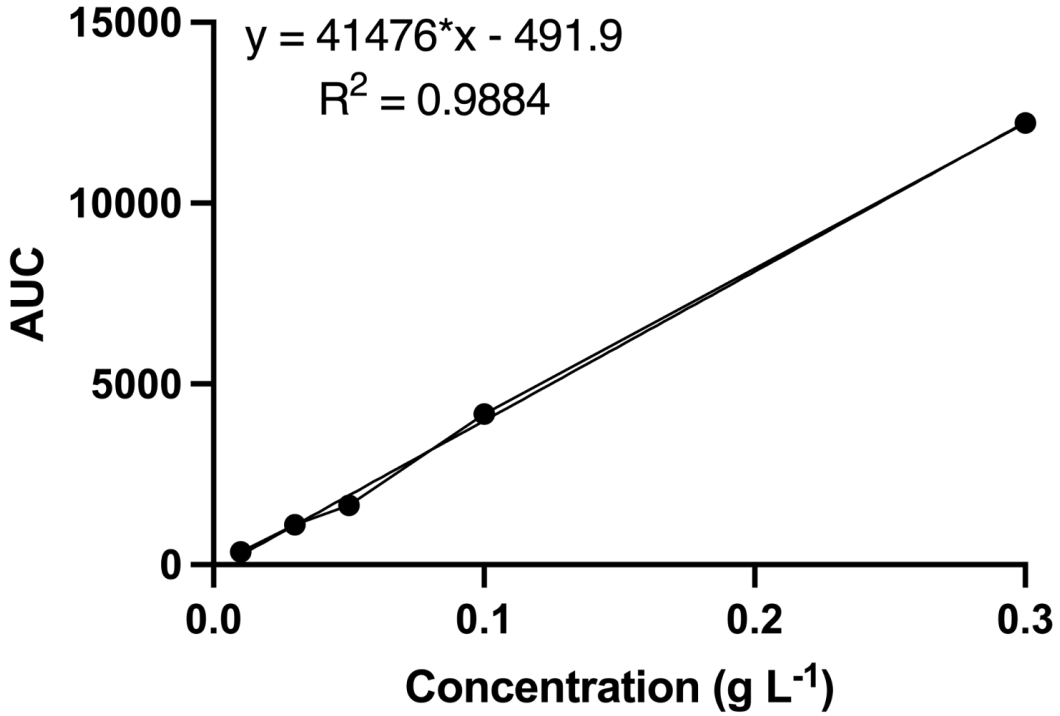

Figure S7. Standard curve of ergothioneine generated via HPLC-DAD.

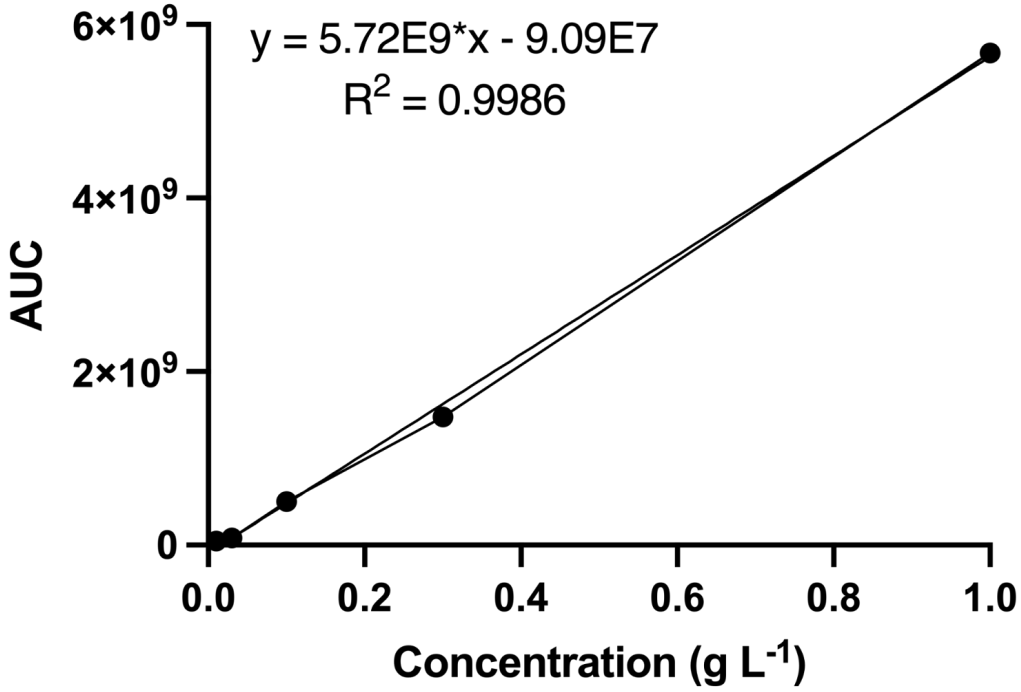

Figure S8. Standard curve of pleuromutilin generated via HPLC-DAD-MS.

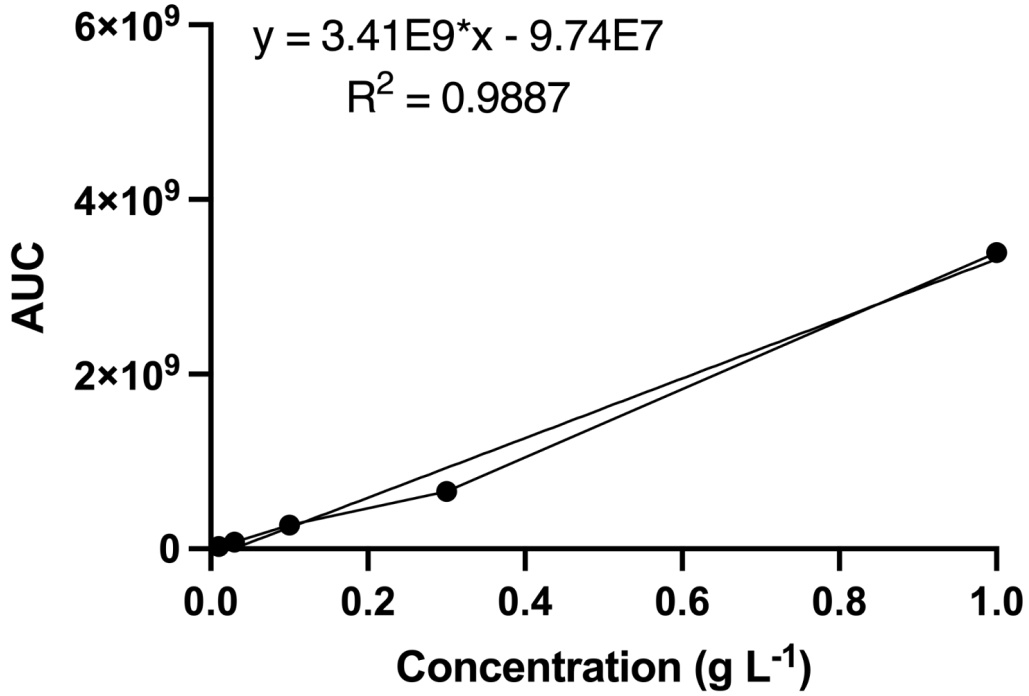

Figure S9. Standard curve of mutilin generated via HPLC-DAD-MS.

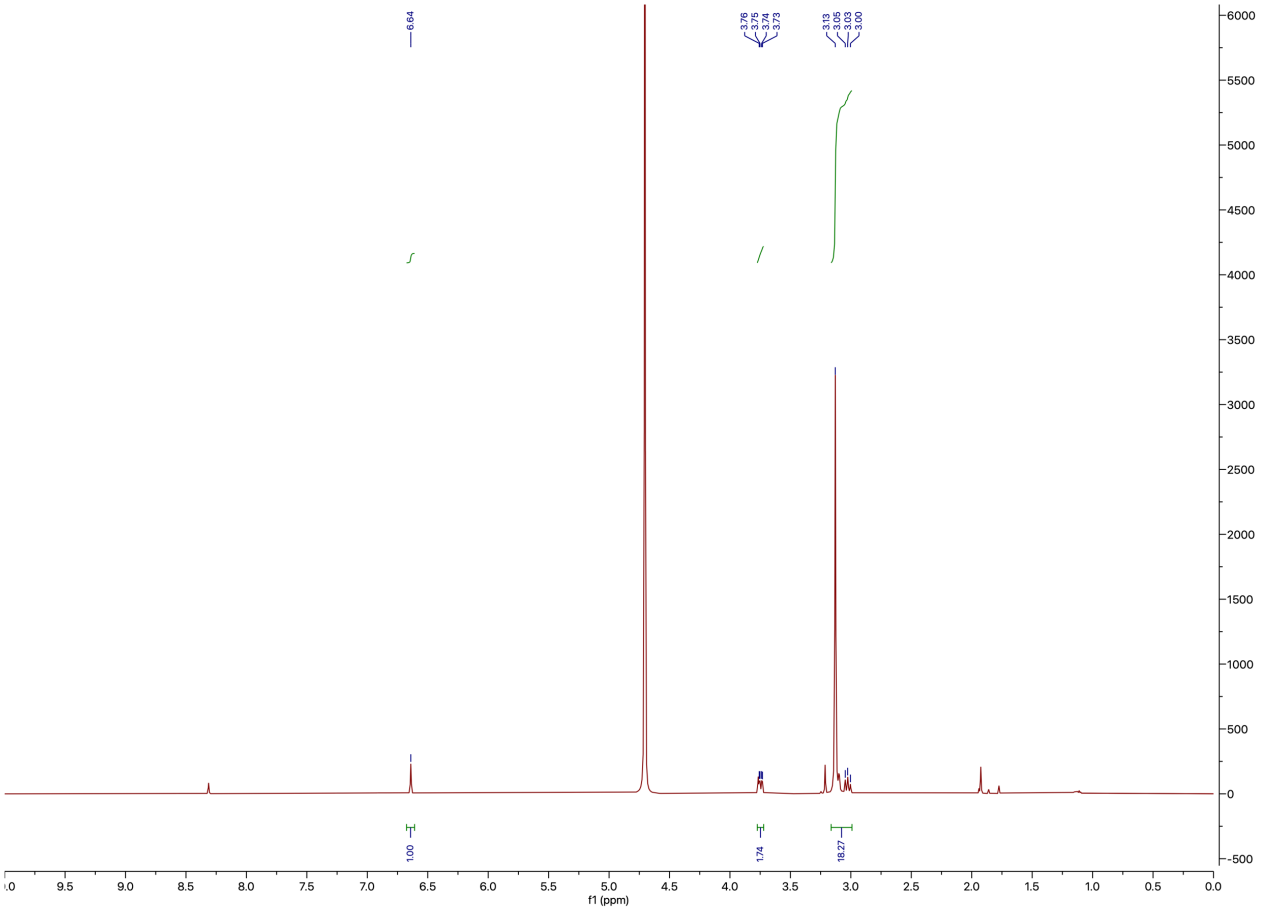

Figure S10. ^{1}H NMR spectrum of ergothioneine. Solvent = D_2O.

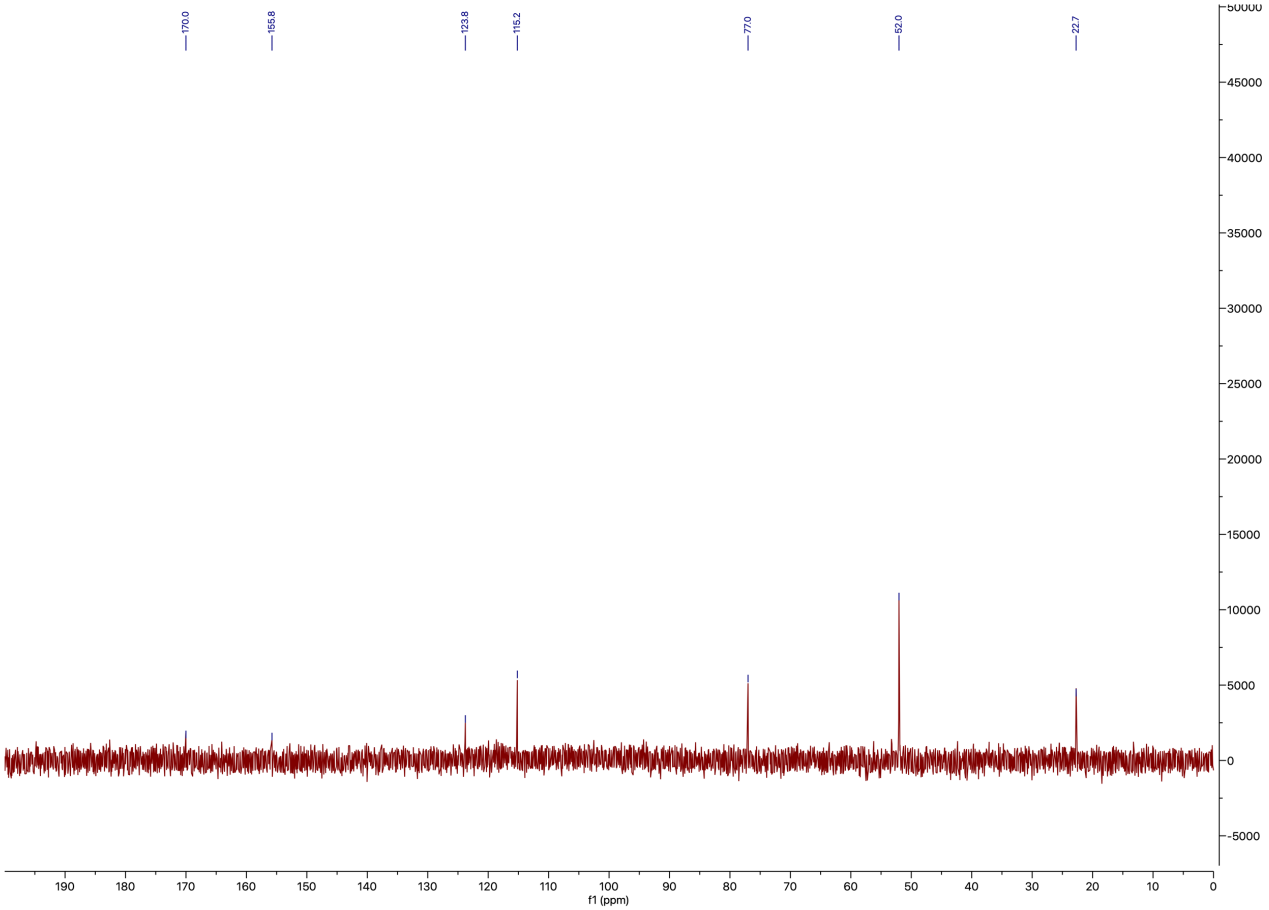

Figure S11. ^{13}C NMR spectrum of ergothioneine. Solvent = D_2O.

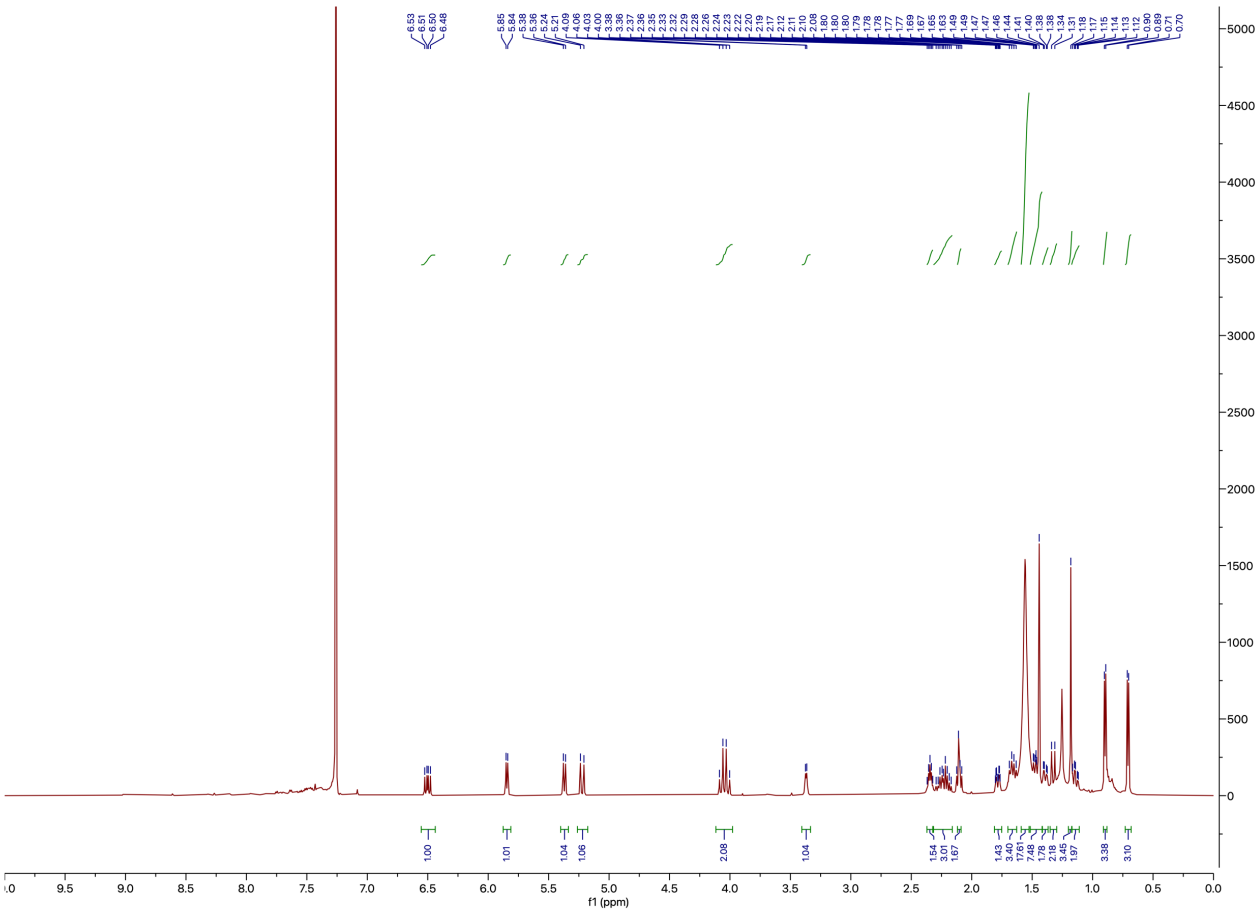

Figure S12. ^{1}H NMR spectrum of pleuromutilin. Solvent = chloroform-*d*.

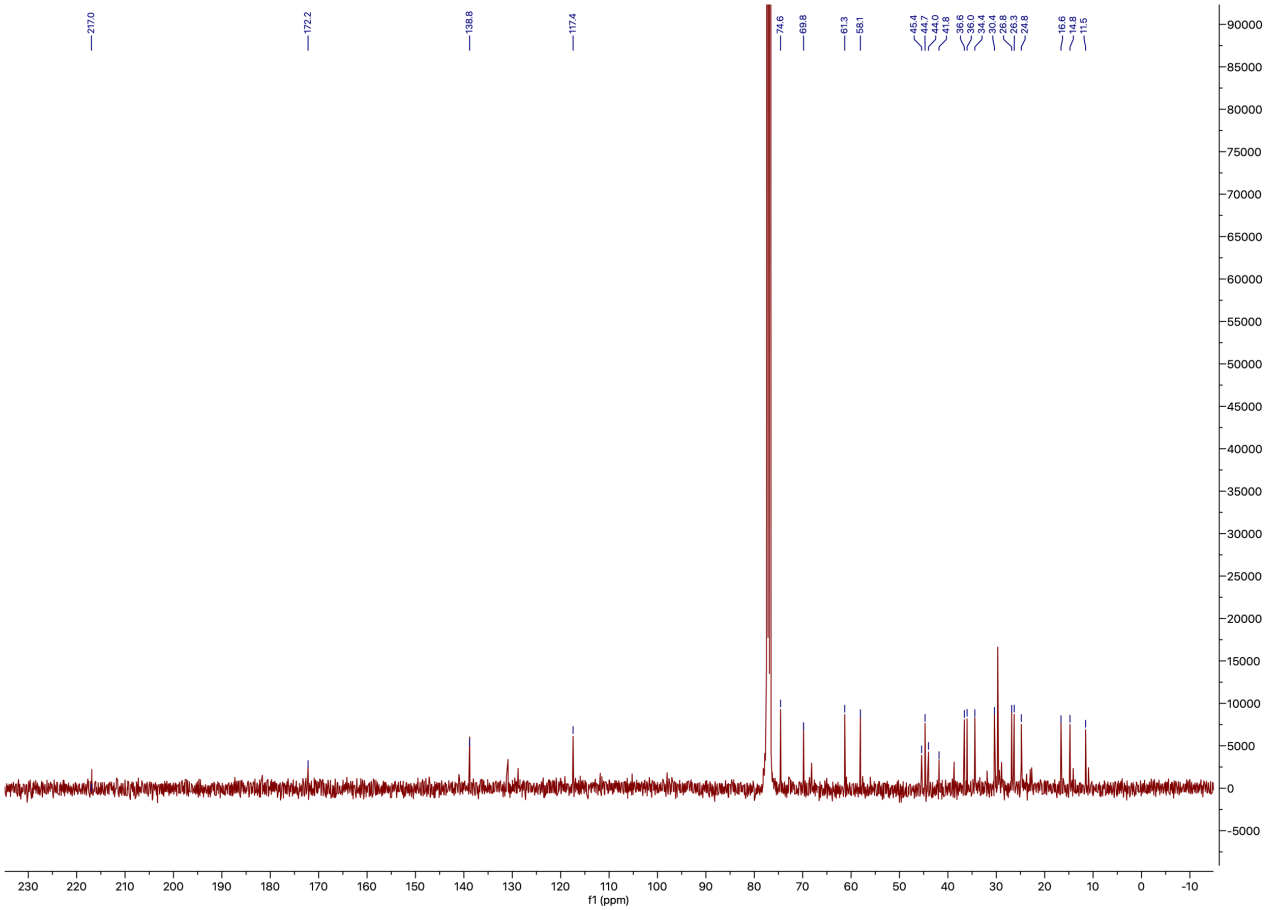

Figure S13. ^{13}C NMR spectrum of pleuromutilin. Solvent = chloroform-*d*.

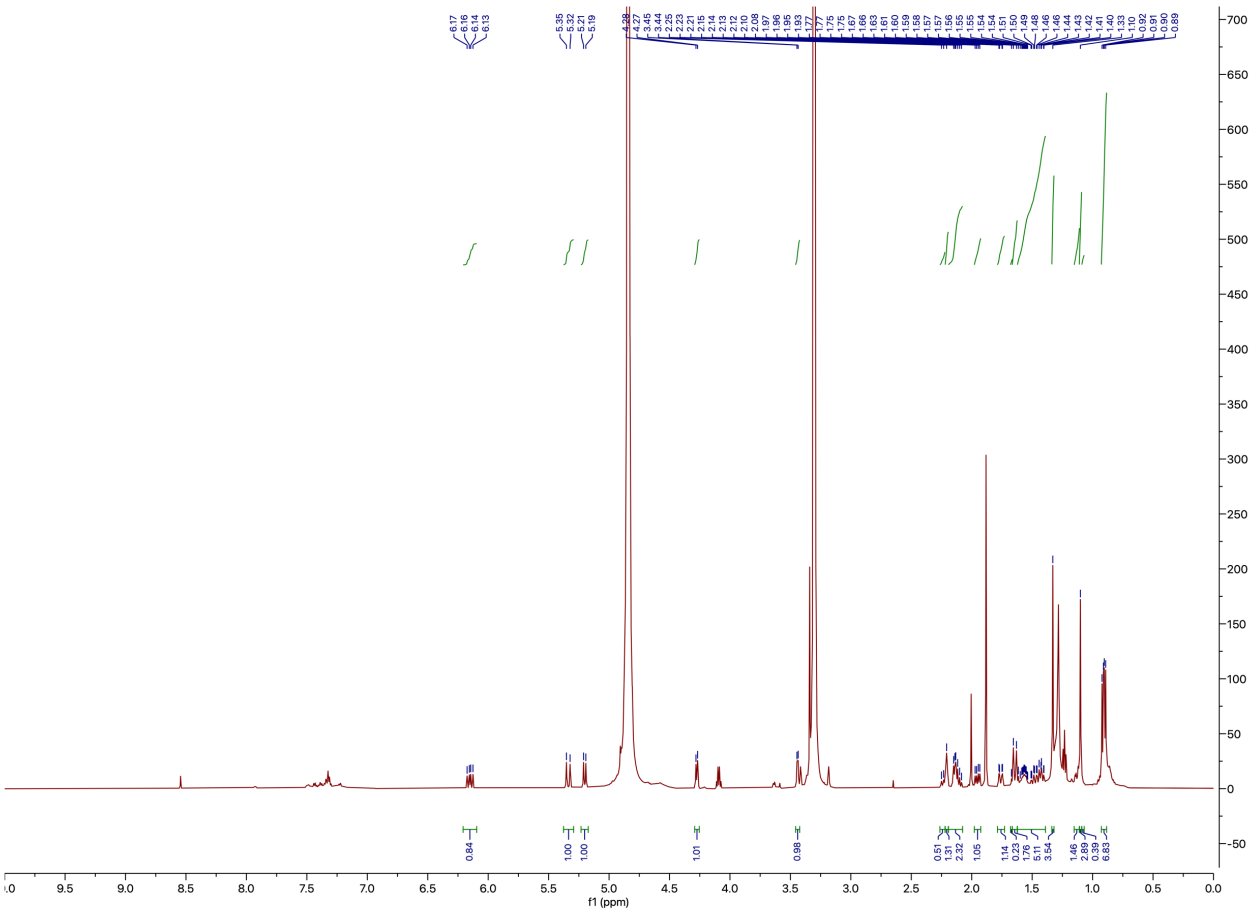

Figure S14. ^{1}H NMR spectrum of mutilin. Solvent = methanol-d_4.

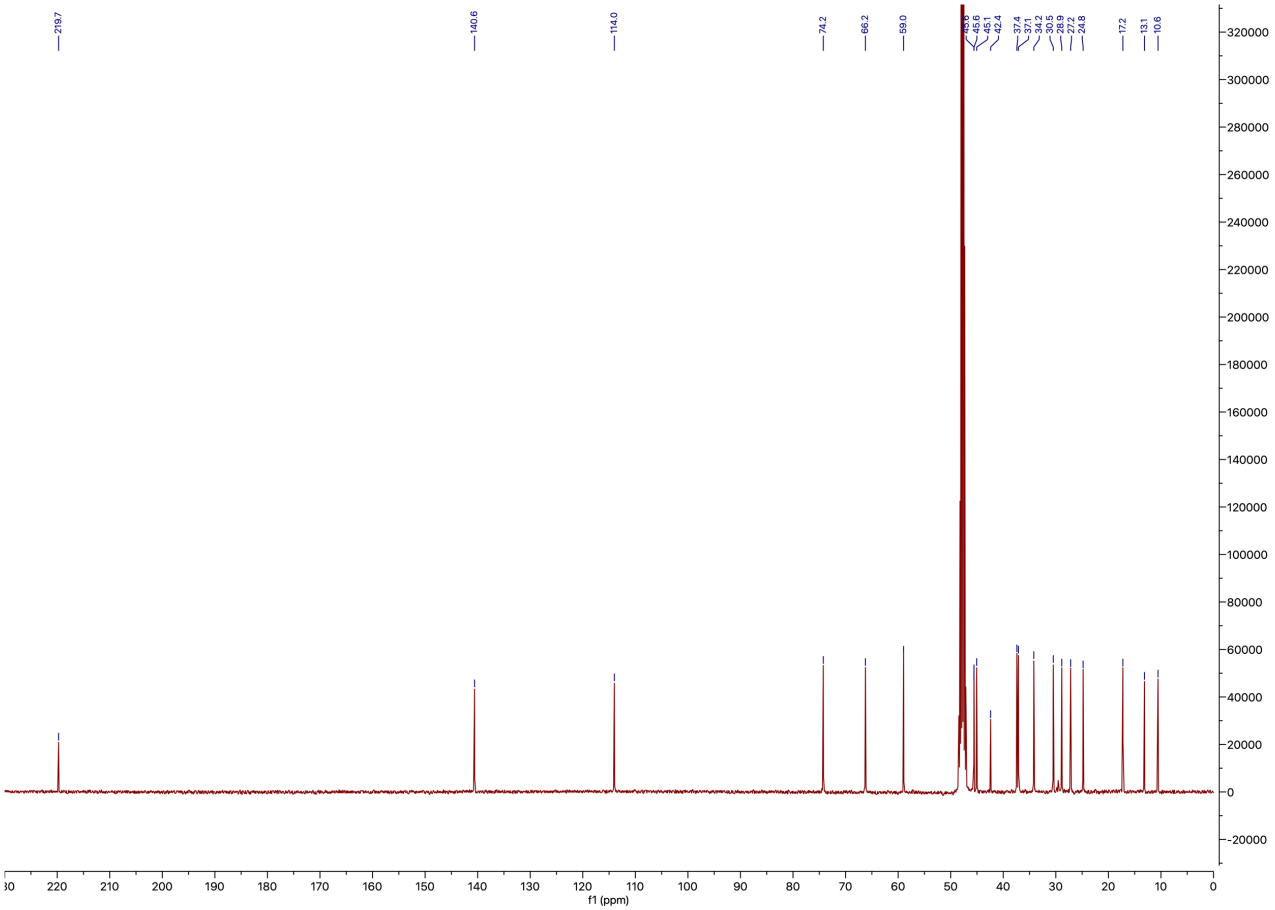

Figure S15. ^{13}C NMR spectrum of mutilin. Solvent = methanol-d_4.

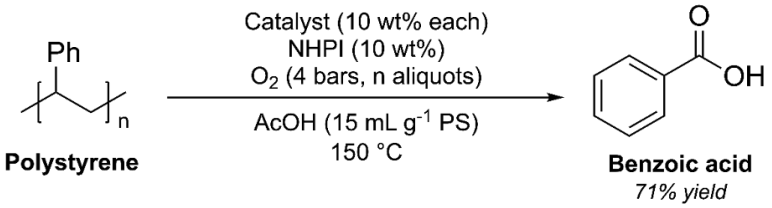

Entry[a]	O_2 Aliquots	O_2 Consumed Equiv[b]	Time (hrs)	Metal Catalyst[c]	Mass Recovery (wt%)[d]	Molar Yield (%)[e]
1	1	0.75	4	$Mn(acac)_3$	3.4	2.8
2	1	0.67	4	$Mn(acac)_2$	4.5	3.8
3	1	0.67	4	$Mn(NO_3)_2$	14.1	12.0
4	1	0.75	4	$Co(NO_3)_2$	6.0	5.1
5	1	0.75	4	$Co(NO_3)_2 + Mn(NO_3)_2$	30.7	26.2
6	2	1.50	8	$Co(NO_3)_2 + Mn(NO_3)_2$	54.6	46.5
7	3	2.06	12	$Co(NO_3)_2 + Mn(NO_3)_2$	84.1	71.4
8	1	0.75	3	$Co(NO_3)_2 + Mn(NO_3)_2$	19.2	16.3
9	2	1.50	6	$Co(NO_3)_2 + Mn(NO_3)_2$	47.2	40.1
10	3	1.98	9	$Co(NO_3)_2 + Mn(NO_3)_2$	72.5	61.5

Table S1. Screening of different catalytic conditions for PS degradation (PS source: waste styrofoam cold box). (a) In a 300-mL Parr reactor, a mixture of PS (5 g), metal catalyst (10 wt%), *N*-Hydroxyphthalimide (NHPI, 10 wt%) and acetic acid (75 mL) was stirred with molecular oxygen (4 bars, with active refilling) at 150 ^oC (b) Equivalents of O_2 per monomer unit in PS (c) Either 0.5 g of one catalyst or 0.25 g of two catalysts (d) Mass recovery yield (wt%) = [(mass of benzoic acid products)/(mass of starting PS)] x 100% (e) molar yield (%) = [(mass of carbon in BA products)/(mass of carbon in starting PS)] x 100%.

Entry	O_2 Aliquots	O_2 Consumed Equiv.	Time (hrs)	Mass Recovery (wt%)	Molar Yield (%)
1[a]	3	2.06	12	84.1	71.4
2[b]	3	1.80	12	60.2	51.1
3[c]	3	1.89	12	45.7	38.8
4[d]	2	1.23	8	17.6	15.0
5[e]	2	1.32	8	25.2	21.4

Table S2. The production of benzoic acid from the degradation of various post-consumer PS waste sources under optimized conditions (entry 7 in table S1). (a) Styrofoam cold box; (b) Styrofoam plate; (c) Catalina Island waste; (d) Coffee lid; (e) Red drink cup.

δ_H (literature) (ppm)	Splitting pattern	*J* (Hz)	δ_H (experimental) (ppm)	Splitting pattern	*J* (Hz)	$\Delta\delta_H$ (ppm)
2.99 - 3.16	m	-	2.99 - 3.16	m	-	0.00
3.73	dd	3.9, 11.7	3.74	dd	3.6, 11.8	0.01
6.64	s	-	6.64	s	-	0.00

Table S3. ^{1}H NMR chemical shifts of ergothioneine compared to literature values[4]. Solvent = D_2O.

δ_C (literature) (ppm)	δ_C (experimental) (ppm)	$\Delta\delta_C$ (ppm)
22.7	22.7	0.0
52.0	52.0	0.0
77.0	77.0	0.0
115.2	115.2	0.0
123.8	123.8	0.0
155.8	155.8	0.0
170.0	170.0	0.0

Table S4. ^{13}C NMR chemical shifts of ergothioneine compared to literature values[4]. Solvent = D_2O.

δ_H (literature) (ppm)	Splitting pattern	*J* (Hz)	δ_H (experimental) (ppm)	Splitting pattern	*J* (Hz)	$\Delta\delta_H$ (ppm)
1.41 - 1.52	m	-	1.42 - 1.52	m	-	0.00
1.61 - 1.73	m	-	1.61 - 1.72	m	-	0.00 - 0.01
2.16 - 2.30	m	-	2.16 - 2.30	m	-	0.00
2.16 - 2.30	m	-	2.16 - 2.30	m	-	0.00
2.11	s	-	2.11	s	-	0.00
1.61 - 1.73	m	-	1.63 - 1.70	m	-	0.02 - 0.03
1.55	dd	13.8, 2.7	1.57	m	-	0.02
1.40	ddd	13.8, 6.0, 2.7	1.39	m	-	0.01
1.79	dq	14.5, 3.1	1.78	dq	14.4, 3.2	0.01
1.15	td	14.3, 4.4	1.14	td	14.2, 4.5	0.01
2.29 - 2.40	m	-	2.31 - 2.37	m	-	0.02 - 0.03
3.34	dd	10.8, 6.6	3.37	d	6.6	0.03
2.10	dd	16.0, 8.7	2.10	dd	16.0, 8.7	0.00
1.33	d	16.0	1.33	d	16.1	0.00
5.85	d	8.6	5.84	d	8.6	0.01
1.44	s	-	1.44	s	-	0.00
0.71	d	7.1	0.71	d	7.1	0.00
0.90	d	7.1	0.90	d	7.1	0.00
1.19	s	-	1.18	s	-	0.01
6.50	dd	17.4, 11.0	6.50	dd	17.4, 11.0	0.00
5.37	dd	11.0, 1.3	5.37	dd	11.0, 1.5	0.00
5.22	dd	17.4, 1.4	5.22	dd	17.4, 1.5	0.00
4.05	qd	17.1, 5.4	4.04	q	17.0, 5.5	0.01

Table S5. ^{1}H NMR chemical shifts of pleuromutilin compared to literature values[5]. Solvent = chloroform-*d*.

δ_C (literature) (ppm)	δ_C (experimental) (ppm)	$\Delta\delta_C$ (ppm)
11.5	11.5	0.0
14.8	14.8	0.0
16.6	16.6	0.0
24.8	24.8	0.0
26.3	26.3	0.0
26.8	26.8	0.0
30.4	30.4	0.0
34.4	34.4	0.0
36.0	36.0	0.0
36.6	36.6	0.0
41.8	41.8	0.0
44.0	44.0	0.0
44.7	44.7	0.0
45.4	45.4	0.0
58.1	58.1	0.0
61.3	61.3	0.0
69.8	69.8	0.0
74.6	74.6	0.0
117.4	117.4	0.0
138.8	138.8	0.0
172.2	172.2	0.0
216.9	217.0	0.1

Table S6. ^{13}C NMR chemical shifts of pleuromutilin compared to literature values[6]. Solvent = chloroform-*d*.

δ_H (literature) (ppm)	Splitting pattern	*J* (Hz)	δ_H (experimental) (ppm)	Splitting pattern	*J* (Hz)	$\Delta\delta_H$ (ppm)
1.27 - 1.70	m	-	1.29 - 1.68	m	-	0.02
1.07 - 1.16	m	-	1.07 - 1.15	m	-	0.00 - 0.01
2.06 - 2.27	m	-	2.08 - 2.26	m	-	0.02 - 0.01
2.20	s	-	2.21	s	-	0.01
1.72 - 1.78	m	-	1.73 - 1.79	dq	14.6, 3.1	0.01
1.27 - 1.70	m	-	1.29 - 1.68	m	-	0.02
1.07 - 1.16	m	-	1.07 - 1.15	m	-	0.00 - 0.01
1.27 - 1.70	m	-	1.29 - 1.68	m	-	0.02
1.07 - 1.16	m	-	1.07 - 1.15	m	-	0.00 - 0.01
2.14	m	-	2.17	m	-	0.03
3.44	d	6.1	3.44	d	6.2	0.00
1.95	d	15.8, 7.6	1.95	dd	15.8, 7.7	0.00
1.64	d	15.8	1.64	d	15.7	0.00
4.27	d	7.6	4.27	d	7.7	0.00
1.33	s	-	1.33	s	-	0.00
0.90	d	7.3	0.90	d	7.2	0.00
0.91	d	7.0	0.92	d	7.0	0.01
1.10	s	-	1.10	s	-	0.00
6.15	dd	17.8, 11.2	6.15	dd	18.0, 11.3	0.00
5.34	dd	17.8, 1.4	5.32	dd	18.0, 1.5	0.02
5.20	dd	11.2, 1.4	5.20	dd	11.2, 1.5	0.00

Table S7. ^{1}H NMR chemical shifts of mutilin compared to literature values[5]. Solvent = methanol-d_4.

δ_C (literature) (ppm)	δ_C (experimental) (ppm)	$\Delta\delta_C$ (ppm)
11.3	10.6	0.7
13.4	13.1	0.3
18.2	17.2	1.0
25.1	24.8	0.3
27.1	27.2	0.1
28.5	28.9	0.4
30.4	30.5	0.1
34.4	34.2	0.2
36.4	37.1	0.7
36.8	37.4	0.6
42.3	42.4	0.1
45.0	45.1	0.1
45.2	45.6	0.4
45.4	45.6	0.2
59.1	59.0	0.1
66.8	66.2	0.6
75.1	74.2	0.9
115.9	114.0	1.9
139.3	140.6	1.3
217.6	219.7	2.1

Table S8. ^{13}C NMR chemical shifts of mutilin compared to literature values[6]. Solvent = methanol-d_4.

Compound	*m/z* (calculated)	*m/z* (found)	Formula	Adduct
Ergothioneine	230.09632	230.09482	$C_9H_{16}O_2N_3S$	$[M + H]^+$
Pleuromutilin	401.23040	401.23093	$C_{22}H_{34}O_5Na$	$[M + Na]^+$
Mutilin	321.24297	321.24304	$C_{20}H_{33}O_3$	$[M + H]^+$

Table S9. High-resolution mass data for ergothioneine, pleuromutilin, and mutilin.

References

1. Osterberg, P. M., Niemeier, J. K., Welch, C. J., Hawkins, J. M., Martinelli, J. R., Johnson, T. E., Root, T. W., & Stahl, S. S. (2015). Experimental Limiting Oxygen Concentrations for Nine Organic Solvents at Temperatures and Pressures Relevant to Aerobic Oxidations in the Pharmaceutical Industry. *Organic Process Research & Development*, *19*(11), 1537–1543. https://doi.org/10.1021/op500328f
2. Hutner, S. H., Provosoli, L., Schatz, A., & Haskins, C. P. (1950). Some approaches to the study of the role of metals in the metabolism of microorganisms. *Proceedings American Phil Society* 94*(2)*, 152–170.
3. Szewczyk, E., Nayak, T., Oakley, C. E., Edgerton, H., Xiong, Y., Taheri-Talesh, N., Osmani, S. A., & Oakley, B. R. (2006). Fusion PCR and gene targeting in *Aspergillus nidulans*. *Nature Protocols*, *1*(6), 3111–3120. https://doi.org/10.1038/nprot.2006.405
4. Hu, W., Song, H., Sae Her, A., Bak, D. W., Naowarojna, N., Elliott, S. J., Qin, L., Chen, X., & Liu, P. (2014). Bioinformatic and Biochemical Characterizations of C–S Bond Formation and Cleavage Enzymes in the Fungus *Neurospora crassa* Ergothioneine Biosynthetic Pathway. *Organic Letters*, *16*(20), 5382–5385. https://doi.org/10.1021/ol502596z
5. Chiang, Y.-M., Lin, T.-S., Chang, S.-L., Ahn, G., & Wang, C. C. C. (2021). An *Aspergillus nidulans* Platform for the Complete Cluster Refactoring and Total Biosynthesis of Fungal Natural Products. *ACS Synthetic Biology*, *10*(1), 173–182. https://doi.org/10.1021/acssynbio.0c00536
6. Fazakerley, N. J., Helm, M. D., & Procter, D. J. (2013). Total Synthesis of (+)-Pleuromutilin. *Chemistry - A European Journal*, *19*(21), 6718–6723. https://doi.org/10.1002/chem.201300968